Post-print of the article published in Desalination:
M. Micari, M. Moser, A. Cipollina, B. Fuchs, B. Ortega-Delgado, A. Tamburini, G. Micale, Techno-economic assessment of multi-effect distillation process for the treatment and recycling of ion exchange resin spent brines, Desalination, Volume 456, 2019, Pages 38-52, https://doi.org/10.1016/j.desal.2019.01.011

Techno-economic Assessment of Multi-Effect Distillation Process for the Treatment and Recycling of Ion Exchange Resin Spent Brines

M. Micari[1], M. Moser[1]*, A. Cipollina[2], B. Fuchs[1], B. Ortega-Delgado[2], A. Tamburini[2]*, G. Micale[2]

1 German Aerospace Center (DLR), Institute of Engineering Thermodynamics, Pfaffenwaldring 38-40, 70569 Stuttgart, Germany
2 Dipartimento dell'Innovazione Industriale e Digitale (DIID), Università degli Studi di Palermo (UNIPA), viale delle Scienze Ed. 6, 90128 Palermo, Italy
*corresponding authors. E-mail: alessandro.tamburini@unipa.it; massimo.moser@dlr.de

Abstract

A treatment chain including nanofiltration, crystallization and multi-effect distillation (MED) is for the first time proposed for the treatment of an effluent produced during the regeneration of Ion Exchange resins employed for water softening. The goal is to recover the minerals and to restore the regenerant solution to be reused in the next regeneration cycle. MED is the most crucial unit of the treatment chain from an economic point of view. A techno-economic analysis on the MED unit was performed and a novel performance indicator, named Levelized Brine Cost, was introduced as a measure of the economic feasibility of the process. Different scenarios were analysed, assuming different thermal energy sources and configurations (plane-MED or MED-TVC). It was found that the plane-MED fed by waste-heat at 1bar is very competitive, leading to a reduction of 50% of the fresh regenerant current cost. Moreover, the thermal energy cost of 20US$/MWh$_{th}$ was identified as the threshold value below which producing regenerant solution in the MED is economically more advantageous than buying a fresh one. Overall, MED allows reducing the environmental impact of the industrial process and it results competitive with the state of the art for a wide range of operating conditions.

Keywords

Industrial brines, Multi-Effect Distillation, Circular Economy, Techno-economic analysis, Brine recycling

1. Introduction and literature review

The disposal of polluted brines coming from industrial processes constitutes a very critical environmental issue of our time. Industrial brines are water solutions, containing sodium chloride, magnesium and calcium salts and, eventually, organic pollutants, released as a waste by several industrial processes. Even the brine generated as by-product by desalination processes has adverse environmental effects if discharged into the sea, because of the higher specific weight of the concentrated brine and the potential presence of additional chemicals [1]. Conventional approach consists in disposing brines directly to water bodies or in injecting them to inland wells [2]. Several studies were conducted to improve the disposal methods and to reduce the environmental impact. In particular, the position of the brine outlet [3] and the possibility to mix the concentrate brine with wastewater or exhaust cooling water [4] were investigated. Currently, some strategies are proposed to treat the brines with a combination of an evaporator with a crystallizer (Zero Liquid Discharge schemes) [5–7]. These strategies allow producing water at a very high purity, but the remaining solid by-product, given by the mixture of different components, is generally a waste, which has to be disposed. In order to tackle this problem and to reduce the disposal requirements, it is possible to develop treatment chains, given by the combination of different processes suitable to treat industrial brines by recovering each of their components. A properly selected treatment chain may lead to the recovery of the valuable products from the brine and to the minimization of the energy requirement of the process, making the brines a source of raw materials, such as water, NaCl and minerals. The definition of the most suitable processes and the process combination in a treatment chain depends on several factors, namely the reject brine volume, the chemical composition, the geographical position of the plant, the feasibility of the process based on the capital and operating costs, the availability of storage and transportation of the brine [6]. In particular, the brine composition strictly depends on the industrial process, which produces the brine. Several industrial processes can be accounted, e.g. desalination and demineralization plants, textile industry and coal mining industry. Many studies were conducted to identify the composition of the brines in the different cases and the possible processes to treat them [7–11]. For example, the brine coming from the textile industry is rich

of organic components, while the brine coming from desalination plants is rich of bivalent ions, such as Mg^{++} and Ca^{++} [11]. With regard to the brine coming from Reverse Osmosis (RO) desalination processes, the profitability of different possible scenarios were compared taking into account the cost of the fresh-water production and the produced salt sale. Drioli et al. investigated the performances of a Microfiltration, Nanofiltration and Reverse Osmosis (MF-NF-RO) membrane system, integrated with a membrane crystallizer, which is employed to bring the RO-concentrate above its saturation limit and to generate NaCl crystal nucleation and growth [12].

Another possible strategy of wastewater treatment consists in producing a water solution, at a defined composition, which can be used as a reactant in the industrial process itself. This approach is commonly used in the textile industry, where the contaminated waste stream is treated via oxidation processes and then re-used for next dyeing operations [13]. Ion Exchange resins operations is another industrial sector where this approach is employed. Ion-exchange resins (IEXs) are often employed for purification (e.g for the removal of nitrates or perchlorates) or for water softening purposes [14]. Spent IEX resins are usually regenerated via the employment of a regenerant solution which is capable of reversing the ion-exchange equilibrium, displacing the ions removed from the treated solution [15]. For the case of demineralization, strong acids like HCl or H_2SO_4 are employed for the regeneration, conversely, in the case of water softening, the regenerant is typically a NaCl-water solution at a concentration ranging between $8\%^{w/w}$ and $12\%^{w/w}$, usually around $10\%^{w/w}$ [16]. During the regeneration, a wastewater solution enriched in the components displaced from the resin is produced. A proper combination of treatment processes allows restoring the regenerant solution required for the regeneration process, starting from the effluent itself. Some studies aimed at closing the loop and reusing the effluent coming from the IEX regeneration to reduce the amount of fresh regenerant solution. Wadley et al. modelled a NF unit used to separate the colorants from the regeneration effluent produced by an IEX in a sugar decolourisation plant [17]. In this case, the employed regenerant solution was a NaCl-water solution ($10\%^{w/w}$) and according to the presented process scheme, the NF permeate was mixed with a make-up NaCl-water solution and then sent back to the IEX as the regenerant. Moreover, IEX technology is widely used to remove pollutants from groundwater, especially nitrate which is the most common contaminants of groundwater and of drinking water sources [18]. The regeneration of the exhaust resins is carried out through a regenerant rich of sodium chloride or sodium bicarbonate, which, at the end of the regeneration process, is enriched of nitrate. Van der Hoek et al. suggested employing a biological denitrification reactor to carry out a

regeneration in a closed circuit [19]. Lehman et al. tested a biological enhanced treatment system to remove both perchlorate and nitrate from the spent IEX brine [20]. Choe et al. investigated the applicability and the environmental sustainability of a catalytic reduction technology for treating nitrate in spent IEX brine [21]. Other studies focused on the recovery of the regenerant solution, for the case of IEX used for water purification from Natural Organic Matters (NOM). The study from Kabsch-Korbutowicz et al. was devoted to assessing the performances of pressure or electrically driven membrane processes in the removal of NOM from the spent IEX regenerant, in order to reuse it for the regeneration process [22]. Finally, Gryta et al. evaluated the employment of a Membrane Distillation (MD) unit for the concentration of IEX effluents with or without a preliminary treatment to avoid the scaling of the membranes [23]. In this case, the solution was concentrated up to the saturation point, to separate the salt crystals.

Ion Exchange resins are also widely used in water softening plants. In this case, the spent regenerant brine is rich of Mg^{++} and Ca^{++}, at a concentration of around 3,000 and 12,500 ppm respectively, while the concentration of nitrate and other species is negligible [24]. This brine has a very low concentration of NaCl (between 10,000 and 15,000 ppm), since a very strong dilution is required to flash out all the high-density spent brine from the softener. A possible treatment chain suitable for this case is reported in Figure 1. This has been developed within the framework of the EU-funded project Zero Brine [25], whose goal is the development of pilot plants able to treat different kinds of industrial brines. In particular, the one schematically represented in Figure 1 is devoted to treating the brine produced in the softening section of the EVIDES company plant, in the Rotterdam port (The Netherlands). In this case, a NF stage is employed to separate most of the bivalent ions. Then, the retentate of the NF stage, rich of Mg^{++} and Ca^{++}, is processed in a crystallization section, where magnesium hydroxide and calcium hydroxide are precipitated and recovered. Conversely, the permeate of the NF stage, rich of NaCl, together with the liquid stream from the crystallization section, is sent to a Multi-Effect Distillation (MED) unit. In this stage, the NaCl-water solution is concentrated up to the required regenerant concentration.

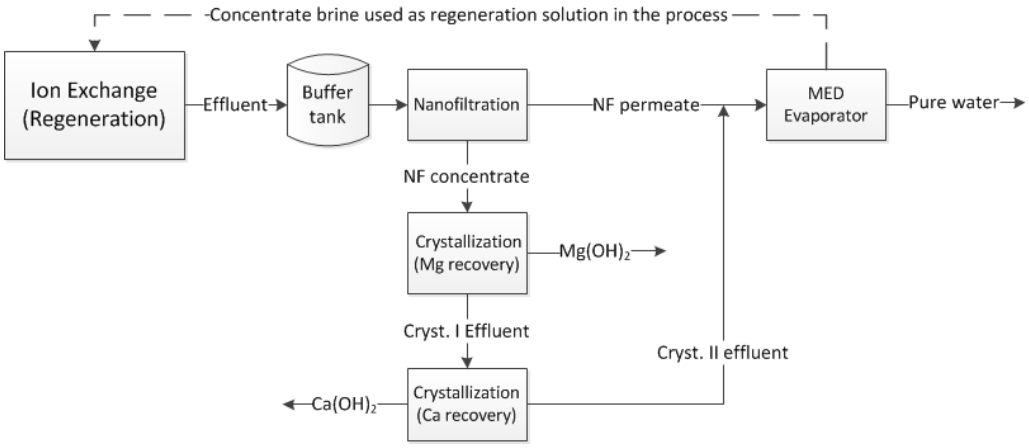

Figure 1. Block Flow Diagram of the proposed treatment chain for industrial brines rich of bivalent ions, coming from Ion Exchange resins regeneration.

MED can play a key role in the treatment of the IEX brines. MED process found a very large application in the desalination field, but there is still room for further investigation of this process in a higher range of feed salinity and brine salinity. Moreover, the presence of a NF stage before the MED can ensure the separation of the bivalent ions. Consequently, the risk of scaling in the heat exchangers, occurring usually with seawater at temperatures higher than 70°C, is negligible and higher Top Brine Temperatures and higher steam temperatures are allowed. In literature, several efforts were made to investigate the coupling of a NF unit with thermal or membrane desalination processes, in order to reduce the risk of scaling due to the presence of hardness in seawater. With this regard, the idea to couple a NF pretreatment step with the traditional thermal or membrane desalination process was firstly proposed by the Saline Water Conversion Corporation (SWCC) [26]. Then, many studies proposed NF-RO, NF-MSF or NF-MED couplings, where the employment of the NF stage allowed a net reduction of the energy and the chemicals consumption of the desalination process [27–31]. Finally, Al-Rawajfeh investigated the possibility to employ a NF unit as CO_2 deaerator to pretreat the feed of a MSF distiller, in order to reduce the alkaline scale formation [32], [33].

In literature, several case studies and several models for the MED plant have been proposed so far. The very first Forward Feed MED (FF-MED) model was proposed by El-Sayed and Silver: it was a design model, relying on some simplified thermodynamic assumptions [34]. Then, El-Dessouki et al. proposed a more sofisticated model for the FF-MED, indicating this arrangement as the most suitable to high temperature application [47]. They also proposed some approximate correlations to calculate the specific heat transfer area, the specific cooling flow rate and the thermal performance ratio as function of the top brine temperature and the number of effects. Kamali et al. presented a model for the MED coupled with a Thermo-

Vapour Compressor (MED-TVC) [35], [36] and Bin Amer et al. developed an optimization tool to maximize the Gain Output Ratio (GOR), varying top brine temperature, entrainment ratio and temperature difference per effect [37]. Recently, Mistry et al. proposed a modular MED model for different flow arrangements, which was compared with the previous models present in literature, showing good agreement and requiring less simplifying assumptions [38]. Finally, Ortega-Delgado et al. developed a detailed model for the FF-MED process and showed a net increase of the perfomance with higher heating steam temperatures [62]. Almost all these models were referred to a desalination process, considering a limited range of concentration and, in some cases, neglecting the influence of some parameters, whose estimation might become very relevant at higher concentration, such as the Boiling Point Elevation (BPE) variation with the composition or the temperature.

Moreover, various economic models were reported in literature for the MED process. Most of these were based on exergy analysis, to identify source and relevance of thermodynamic inefficiencies. Sayyadi et al. proposed an economic model, based on exergy analysis, for a parallel-cross (PC) MED-TVC system, with equal temperature differences for each effect and neglecting the pressure drops in the pipelines [39]. Then, the same authors presented three optimization scenarios: (i) the maximization of the exergy efficiency of the MED-TVC, (ii) the minimization of the cost of the fresh water production, (iii) a combination of the previous two [40]. Esfahani et al. proposed a multi-objective optimization to minimize the total annual costs and maximize the GOR [41]. Recently, Piacentino presented a detailed thermo-economic analysis for the case of a FF-MED plant. The research allowed identifying a cost for each material stream and describing all the single contributions to the final distillate cost [42]. Finally, Papapetrou et al. reviewed the methodologies used in literature for the estimation of the costs in the desalination plants, their range of validity and their limits [60].

In the present work, a fully-integrated techno-economic model for the MED process is presented: in the same simulation, the economic section of the model receives the main inputs directly from the technical model calculations (i.e. size of the equipment and energy requirement) to evaluate the capital and the operating costs, thus providing the final feasibility assessment of the MED technology. The model is applicable to a wide range of input parameters (e.g. feed salinity, steam temperature, number of effects) and able to easily switch between design methods (i.e. equal heat exchanger areas or equal temperature changes in the effects) and between feed flow arrangements (i.e. parallel cross and forward feed). For the first time, the application of the MED process to the treatment of the brines coming from the regeneration of spent IEXs is investigated. This new application of the MED made necessary

to introduce a new parameter to define its performance. This has to be different from the most common performance parameter used for desalination plants, i.e. the Levelized Cost of Water (LCOW). With this aim, the Levelized cost of Brine (LBC) is introduced here for the first time, since the concentrate solution (brine) produced by the MED is the main valuable product of the treatment process. Therefore, the feasibility of this novel application of MED technology is assessed via the comparison of the calculated LBC with the current cost of the regenerant solution, i.e. the cost of a fresh NaCl-water solution for every regeneration cycle. Two scenarios are investigated, with reference to different thermal energy supplies. In the first one, the thermal energy is assumed to be completely provided by a gas turbine co-generation system, with a cost depending on the steam pressure. Conversely, the second scenario provides the utilization of waste heat available in the industrial site, at given quality and cost. In both scenarios, the performances of a plane MED and a MED-TVC are compared and a sensitivity analysis including the number of effects, the steam temperature and the motive steam pressure (for the case of MED-TVC) is carried out. Moreover, once the system configuration has been optimized on the basis of the thermal energy cost, the effects of the electric energy cost and of the revenue coming from the pure water production on the LBC are assessed. Finally, the influence of the feed flow rate on the LBC is assessed, in order to investigate the effect of the economy of scale on the proposed system.

Overall, the present work aims at proposing a new technological solution to treat an industrial wastewater effluent, whose treatment has not been investigated yet in literature and at evaluating the most suitable conditions to operate the MED unit in the treatment chain.

2. Model

2.1 Integrated Techno-economic Model

The techno-economic model is composed of a technical and an economic part that are fully integrated and implemented in Python. The technical/design model is mainly based on mass and energy balances at steady-state conditions and on the evaluation of thermo-physical properties of water, in the liquid or in the vapor state, and of the NaCl-water solution [62]. These properties are estimated via correlations reported in literature. The economic model evaluates the capital costs, via the estimation of the costs of the single equipment, and the operating costs, making reference to the calculated energy requirements. The main input variables for the technical model are: feed salinity, temperature and flow rate, steam temperature, motive steam pressure (in presence of the TVC), required brine salinity, temperature of the last effect and number of effects. All the geometrical features, such as the

size of the tubes in the tube bundles or of the connecting lines, are given as parameters. Conversely, the key output variables of the design model are the heat exchanger areas, the preheater areas and the end-condenser area, the steam flow rate and the motive steam flow rate in the case of the MED-TVC. These variables (along with other financial parameters) constitute the inputs of the economic model, whose results are the annualized capital and operating costs, the revenue from the pure water production and the capital, operating and total Levelized Brine Cost. The most relevant inputs and outputs of the techno-economic model are summarized in Table 1.

The integrated model takes advantage from a purposely developed resolution algorithm which includes minimization steps (via iterative procedures) allowing design requirements to be fulfilled. The model is able to run for different feed arrangements (FF-MED and PC-MED) and different design methods, which refer to different design requirements, i.e. one provides equal heat exchangers area (A_{HX}) and equal preheaters area (A_{preh}) while the other provides equal temperature differences (ΔT_{eff}) for each effect. For the case under investigation, i.e. the concentration of the effluent coming from the IEX resins, the FF arrangement was selected as the most suitable, given the high concentrations which have to be reached and the possibility to employ high Top Brine Temperatures to enhance the performances in absence of TVC [47]. Moreover, for easiness of comparison with other technical models, the design method with equal areas of the heat exchangers and the preheaters was selected.

Table 1. Main inputs and outputs of the technical and the economic model for the MED process.

Model	Inputs	Outputs
Technical model	Number of effects (N [-])	Distillate flow rate (M_{dist} [kg/s])
	Feed flow rate (M_{feed} [kg/s])	Brine flow rate (M_{brine} [kg/s])
	Feed salinity (X_{feed} [ppm])	Heat exchanger areas (A_{HX} [m^2])
	Intake feed temperature (T_{feed} [°C])	Preheater areas (A_{preh} [m^2])
	Brine salinity (X_{brine} [ppm])	End-condenser area (A_{cond} [m^2])
	Steam temperature (T_s [°C])	Cooling-water flow rate (M_{cw} [kg/s])
	Motive steam pressure (P_m [bar])	Steam flow rate (M_s [kg/s]) and motive steam flow rate for MED-TVC (M_m [kg/s])
	Temperature in the last effect (T_N [°C])	Specific area (sA [m^2/(kg/s)]) and specific thermal consumption (sQ [kJ/kg])
Economic	Heat exchanger areas (A_{HX} [m^2])	Annualized capital cost (CAPEX [US$/y])

model	Preheater areas (A_{preh} [m^2])	Annualized operating cost (OPEX [US$/y])
	End-condenser area (A_{cond} [m^2])	Water revenue (R_{wat} [US$/y])
	Cooling-water flow rate (M_{cw} [kg/s])	Capital levelized brine cost (LBC_{CAP} [US$/$m^3$])
	Steam flow rate (M_s [kg/s]) for MED or motive steam flow rate for MED-TVC (M_m [kg/s])	Operating levelized brine cost (LBC_{OP} [US$/$m^3$])
	Electric energy requirement (P_{el} [kWh_{el}/m^3])	Total levelized brine cost (LBC_{tot} [US$/$m^3$])

The structure of the resolution algorithm is reported in Figure 2. As shown in the figure, the technical model presents three minimization loops, since it is required that (i) the areas of the heat exchangers (A_{HX}) and (ii) the areas of the preheaters (A_{preh}) have to be equal and (iii) a given distillate flow rate (M_{dist}) corresponding to a given brine salinity has to be produced. Once all the three requirements are satisfied, the technical results are available and are given as inputs to the economic model. Additional details on both the technical and the economic part of the model are reported in the following sections.

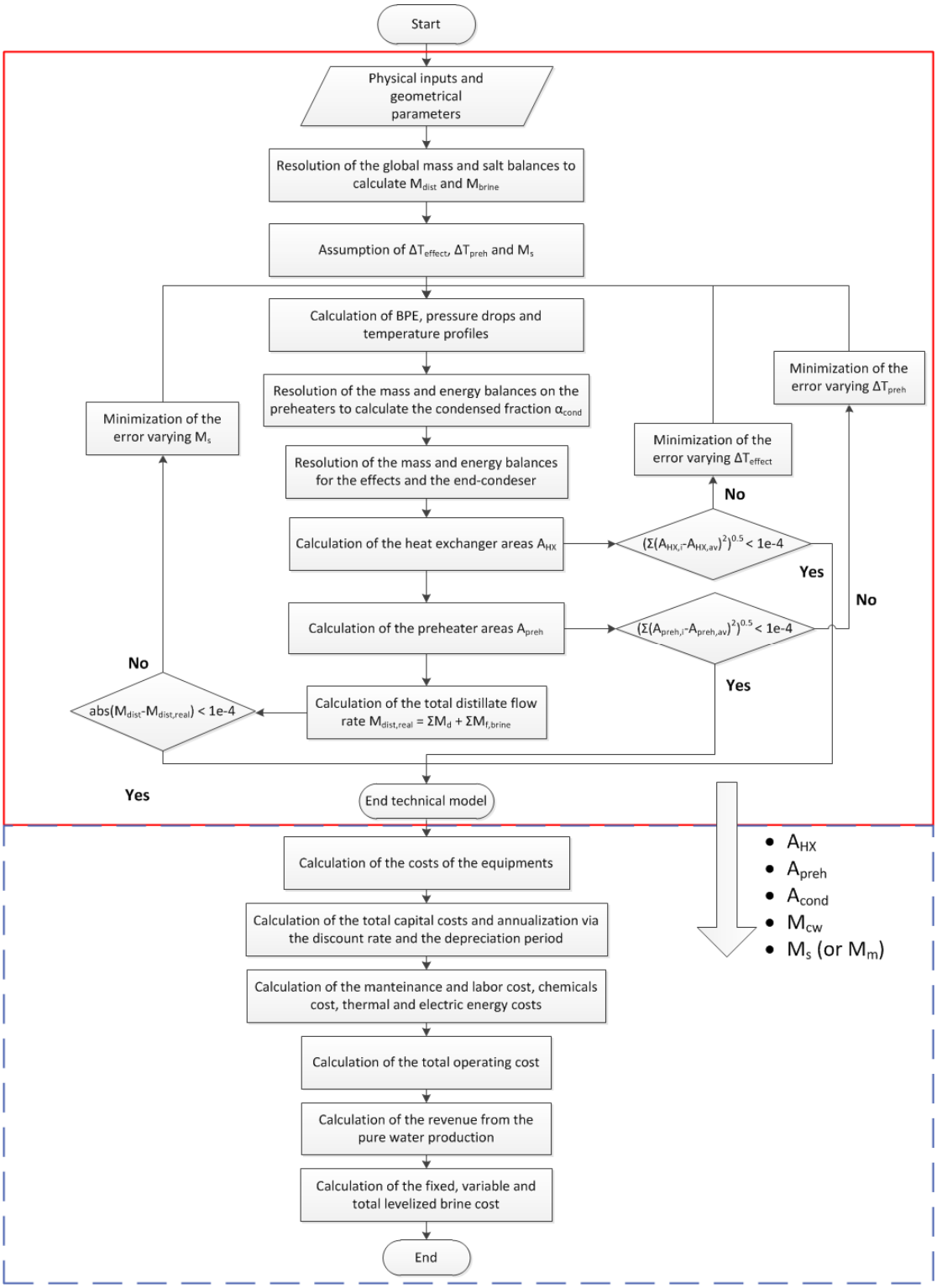

Figure 2. Resolution algorithm for the MED model. The solid red rectangle encompasses the technical model procedure, while the broken blue rectangle contains the economic model one.

2.2 Technical Model

The main output variables are the specific area (sA), the specific thermal consumption (sQ) and the GOR, which are defined as follows.

$$sA = \frac{\sum_N A_{HX} + \sum_{N-1} A_{preh} + A_{cond}}{M_{dist}} \quad (1)$$

$$sQ = \frac{M_s\, \lambda(T_s)}{M_{dist}} \quad (2)$$

$$GOR = \frac{M_s}{M_{dist}} \quad (3)$$

Where $\lambda(T_s)$ is the latent heat of water at a temperature equal to T_s.

A short description and a table containing the main equations of the FF-MED steady-state model used for the simulations are reported in the following.

Forward Feed Model

The schematic representation of the MED plant described in the present FF-MED model is reported in Figure 3. It shows the first effect, a generic intermediate effect and the last effect with the end condenser. In fact, three slightly different systems of mass and energy balance equations are used to model these three classes of effects.

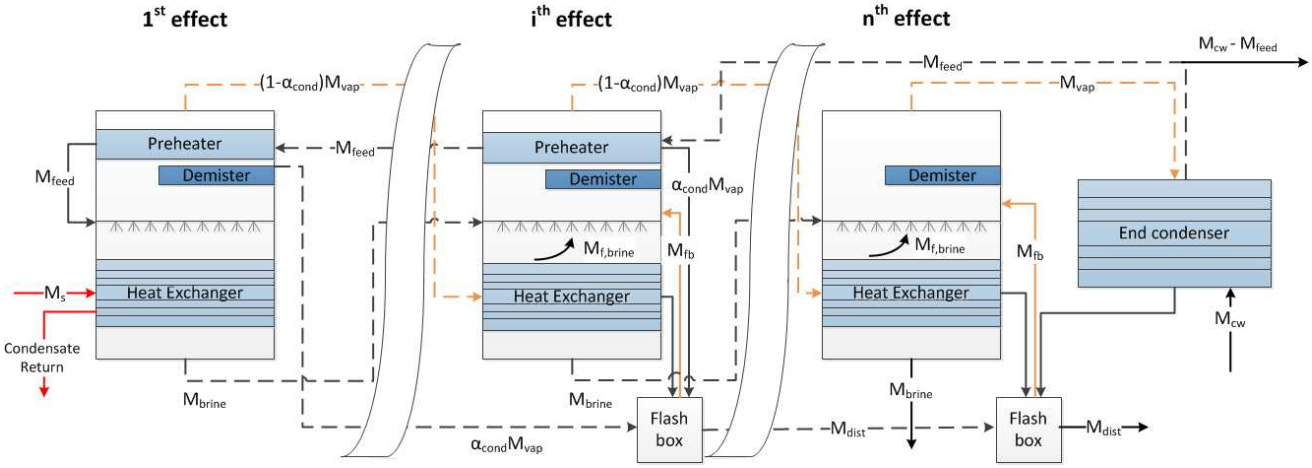

Figure 3. Schematic representation of the MED plant.

All the equations relevant to the model of the FF-MED are reported in Table 2 where λ is the latent heat of water, h_{vap} is the enthalpy of the steam, h_{liq} is the enthalpy of the liquid water, h_{sw} is the enthalpy of the NaCl salt-water solution and $c_{p,sw}$ is the NaCl salt-water solution specific heat. The water properties are function of temperature, while the NaCl-water solution properties are functions of temperature and composition.

Table 2. Main mass and energy balance equations of the forward-feed MED model.

N	Equation	Short description
(4)	$M_{feed} = M_{dist} + M_{brine}$	Global mass balance
(5)	$M_{feed}\, X_{feed} = M_{brine}\, X_{brine}$	Global salt balance
(6)	$T_{vsat} = T - BPE(T,\, X_{brine})$	Temperature drop for the BPE
(7)	$T'_{vsat} = T_{vsat} - \Delta T_{demister}$	Temperature drop in the demister
(8)	$T'_c = T'_{vsat} - \Delta T_{lines}$	Temperature drop in the connecting lines
(9)	$T_c = T'_c - \Delta T_{grav} - \Delta T_{acc}$	Temperature drop in the evaporator
(10)	$M_s\,\lambda(T_s) + M_{feed}\, h_{sw}\big(T_{preh}[1],\, X_{feed}\big) = M_b[1]\, h_{sw}(T[1],\, X_b[1]) + (1-\alpha_{cond}[1])\, M_{vap}[1]\, h_{vap}(T'_{vsat}[1]) + \alpha_{cond}[1] M_{vap}[1]\, h_{liq}(T'_{vsat}[1])$	Energy balance on the first effect
(11)	$M_b[i-1] = M_d[i] + M_{fbrine}[i] + M_b[i]$	Mass balance on a generic effect
(12)	$M_{feed}\, X_{feed} = M_b[i]\, X_b[i]$	Salt balance on a generic effect
(13)	$M_{vap}[i] = M_d[i] + M_{fbrine}[i] + M_{fb}[i]$	Mass balance on the vapor phase
(14)	$M_c[i-1] + \alpha_{cond}[i]\, M_{vap}[i] + (1-\alpha_{cond}[i-1]) M_{vap}[i-1] = M_{fb}[i] + M_c[i]$	Mass balance on the generic flash-box
(15)	$M_c[i-1]\, h_{liq}\big(T'_{v,sat}[i-1]\big) + \alpha_{cond}[i]\, M_{vap}[i]\, h_{liq}(T'_{vsat}[i]) + (1-\alpha_{cond}[i-1]) M_{vap}[i-1]\, h_{liq}(T_c[i-1]) = M_{fb}[i] h_{vap}(T'_{vsat}[i]) + M_c[i] h_{liq}(T'_{vsat}[i])$	Energy balance on the generic flash-box
(16)	$M_{fbrine}[i]\, \lambda\big(T_{brine,\,f}[i]\big) = M_{brine}[i-1]\, c_{P_{sw}}(T_{mean},\, X_b[i-1]) \big(T[i-1] - T_{brine,\,f}[i]\big)$	Energy balance on the brine entering as the feed ($T_{brine,f}$ calculated via the Non Equilibrium Allowance [47])
(17)	$M_{feed}\, c_{P_{sw}}\big(T_{mean},\, X_f\big)\, \big(T_{preh}[i] - T_{preh}[i+1]\big) = \alpha_{cond}[i]\, M_{vap}[i]\, \lambda(T'_{vsat}[i])$	Energy balance on a generic preheater
(18)	$(1-\alpha_{cond}[i-1]) M_{vap}[i-1]\, \lambda(T_c[i-1]) + M_{fbrine}[i]\, \big(h_{sw}(T[i-1], X_b[i-1]) - h_{vap}(T'_{vsat}[i])\big) + M_b[i]\big(h_{sw}(T[i-1], X_b[i-1]) - h_{sw}(T[i], X_b[i])\big) = M_d[i]\, \big(h_{vap}(T'_{vsat}[i]) - h_{sw}(T[i-1], X_b[i-1])\big)$	Energy balance on a generic heat exchanger
(19)	$(1-\alpha_{cond}[N-1]) M_{vap}[N-1]\, \lambda(T_c[N-1]) + M_{fb}[N]\, h_{vap}(T'_{vsat}[N]) + M_b[N-1]\, h_{sw}(T[N-1],\, X_b[N-1]) = M_b[N]\, h_{sw}(T[N],\, X_b[N]) + M_{vap}[N]\, h_{vap}(T'_{vsat}[N])$	Energy balance on the last effect
(20)	$M_{cw}\, c_{P_{sw}}\big(\overline{T_{cw}}, X_{feed}\big)\, \big(T_{cw,out} - T_{cw,in}\big) = M_{vap}[N]\, \lambda(T'_c[N])$	Energy balance on the end condenser

Basically, each run starts from the calculation of global mass and salinity balances, to estimate the brine flow rate (M_{brine}), the distillate flow rate (M_{dist}) and the brine salinity (X_{brine}), under the assumption that the distillate is pure water. Then, all the variables, such as mass flow rate, temperature and pressure, related to each single effect are estimated. Regarding the temperature profiles, six main quantities have to be calculated: temperature of the brine generated in the effect (T), temperature reached by the feed in the preheater of the effect (T_{preh}), temperature of the saturated vapor generated in the effect (T_{vsat}), temperature of the vapor after crossing the demister (T'_{vsat}), temperature of the vapor after crossing the connecting lines (T'_c) and condensation temperature of the vapor in the following effect (T_c). These are interdependent according to the equations (6)-(9), through the boiling point elevation (BPE) and the pressure drops, which lead to temperature drops ($\Delta T_{demister}$, ΔT_{lines}, ΔT_{grav}, ΔT_{acc}), in the case of saturated vapor. The boiling point elevation is estimated through the Pitzer model, which is valid in a wider range of salinity compared to the other correlations in literature [43], [44]. The pressure drops are estimated according to some correlations present in literature [45], [46]. Concerning the modelling of the effects, the first effect is the only one which receives heat from an external source (M_s at temperature equal to T_s) and in which the feed (M_{feed} at a concentration equal to X_{feed}) enters after having crossed all the preheaters. The feed is sprayed on a tube bundle, while M_s flows inside the tubes. In this effect, the vapor generated (M_{vap}) is given only by the partial evaporation of the feed (M_d). This crosses the demister and the first preheater, where it partially condenses. The remaining part is sent to the following effect, as the heating steam. The brine generated in the first effect (M_b at a concentration equal to X_b) is sent to the following effect as the feed, sprayed on the external surface of the tube bundle. The intermediate effects' modelling includes the two energy balances on the preheater and on the heat exchanger to know the condensed fraction on the preheater tube surface (α_{cond}) and M_d, respectively (Equation (17)-(18)). Moreover, other two vapor contributions have to be considered: the vapor generated by the inlet brine flash (M_{fbrine} from equation (16)) and the vapor coming from the flashing box M_{fb}, which is generated by the flash of the condensed distillate collected in the flashing box (M_{fb} and M_c, the condensate exiting from the flash box, are derived from equation (14), (15)). Finally, the last effect differs from the others because it does not have any preheater and the entire vapor generated in the last effect is sent to the end condenser, where it condenses completely. This leads to a slightly different expression of the energy balances on the effect (Equation (19)) and on the last flashing box, since the total M_{vap} generated in the last effect condenses in the end condenser and then is collected in the flash box. The brine generated in the last effect (M_b

[N]) constitutes the final brine produced by the plant, while the condensate exiting from the last flash box (M_c [N]) constitutes the final distillate. These have to satisfy the global balance in Equations (4)-(5). Regarding the end condenser, usually, the feed itself is used to condensate the vapor. The necessary total cooling water flow rate (M_{cw}) is calculated through the heat balance reported in Equation (20) and the surplus ($M_{cw} - M_{feed}$) is cooled down and can be reused.

Finally, the areas of the heat exchangers, of the preheaters and of the end condenser are calculated according to Equations (21)-(24). In these equations, $DTML_{preh}$ and $DTML_{cond}$ are the temperature logarithmic mean in the preheater and in the condenser and U_{cond} and U_{evap} are the heat transfer coefficients for the condenser and the evaporator respectively, derived from correlations by El-Dessouky et al. [47].

Table 3. Equations to calculate the heat exchangers, preheaters and end condenser areas of the MED plant.

N	Equation
(21)	$A_{hx}[0] = \frac{M_{feed} c_{P_{sw}}(T_{mean}, X_f)(T[1] - T_{preh}[1]) + M_d[1]\,\lambda(T_{vsat}[1])}{U_{evap}(T[1])(T_{steam} - T[1])}$
(22)	$A_{hx}[i] = \frac{(1 - \alpha_{cond}[i-1]) M_{vap}[i-1]\,\lambda(T_c[i-1])}{U_{evap}(T[i])(T_c[i-1] - T[i])}$
(23)	$A_{preh}[i] = \frac{\alpha_{cond}[i]\, M_{vap}[i]\ \lambda(T'_{vsat}[i])}{U_{cond}(T'_{vsat}[i])\ DTML_{preh}}$
(24)	$A_{cond} = \frac{M_{cw}\ c_{P_{sw}}(\overline{T_{cw}}, X_{feed})\ (T_{cw,out} - T_{cw,in})}{U_{cond}(T'_c[N])\ DTML_{cond}}$

The described technical model was validated through the comparison with another FF-MED model, which is reported in literature [62]. The results of one of the sensitivity analyses carried out for validation purposes are reported in the Supplementary materials.

Thermo-vapour Compressor

In the case of a MED-TVC system, a certain amount of vapor generated in one effect is recycled to the first effect as part of the heating steam. More in detail, this is possible using a compression device, such as a thermo-compressor, in which a fraction of the vapor coming from the last effect or from an intermediate (i.e. entrained vapor) is mixed with the vapor coming from an external source (i.e. motive steam). In this work, the entrained vapor is always taken from the last effect. The discharged vapor is rejected as super-heated vapor at a

pressure equal to the saturation pressure at $T=T_s$. In order to model the TVC, some correlations reported in literature are employed [48], [56]. Given the pressure of the motive steam P_m, the saturation pressure at T_s (P_s) and the pressure of the entrained vapor (P_{ev}, i.e. the saturation pressure at T_n), it is possible to calculate the compression ratio ($C_R = P_s / P_{ev}$) and the expansion ratio ($ER = P_m / P_{ev}$). Thus, the correlations allow calculating the entrainment ratio ($Ra = M_m / M_{ev}$) and, consequently, the amount of steam which has to be supplied externally (M_m).

2.3 Economic Model

The economic model receives as input parameters the main outputs of the technical model, i.e. the areas of the heat exchangers, the preheaters and the end condenser, the required steam flow rate (M_s for the plane MED system and M_m for the MED-TVC) and the cooling water flow rate. The outputs of the economic model are the capital and the operating costs and the Levelized Brine Cost (LBC).

Capital Costs

The capital costs are evaluated through the module costing technique, described extensively in [52] and widely used in literature as a standard tool for economic assessments of chemical plants [49–51]. This technique estimates the capital cost of every unit included in the process as a function of its purchased cost. The basis purchased cost of each element (C_p^0) is evaluated for some base conditions, i.e. equipment operating at ambient pressure and fabricated from most common material, usually carbon steel. The basis C_p^0 values are reported in database where these refer to a specific unit scale and are relevant to a specific year. The actual C_P^0 values are calculated for all equipment as function of their actual size, i.e. the area in the case of the heat exchangers and the condenser and the volume in the case of the pressure vessels. The C_P^0 values are then actualized through the Chemical Engineering Plant Cost Index (CEPCI). In the case of construction materials different from the ones employed for the base case (usually carbon steel) and pressures different from ambient pressure, suitable correction factors relevant to both purchased and installation costs are estimated for any kind of equipment. Finally, the bare module cost of the equipment C_{BM} is calculated multiplying the C_p^0 by a bare module factor F_{BM}, which takes into account all the above factors, together with the terms of cost related to freight, overhead and engineering:

$$C_{BM} = C_P^{\,0} F_{BM} \tag{25}$$

In this way, it is possible to evaluate the cost of the single effect, considering each effect as the combination of two heat exchangers (i.e. the evaporator and the preheater) and one vessel (i.e. the flash box). Regarding the heat exchangers, these are supposed to have the shell in carbon steel and the tubes in a nickel-based alloy, which has an excellent resistance to saltwater and high temperatures [52], [61]. The total cost of the equipment is calculated as the sum of the costs of the single effect, plus the cost of the end condenser and of the thermo-vapor compressor (for the case of MED-TVC). The estimation of the thermo-vapor compressor cost makes reference to a TVC whose cost and plant size, in terms of produced distillate flow rate, are known [57]. Finally, the total module cost (C_{TM}) is evaluated adding the contingency and fee cost to the cost of equipment, which are commonly assumed as 15% and 3% of the cost of equipment, respectively [52]. The auxiliary facility cost is neglected, since the plant is supposed to be built in an already developed industrial area. The total module cost is annualized (CAPEX in US$/y), through the discount rate (i) and assuming a certain plant lifetime (n_{years}), according to the following definition:

$$CAPEX = C_{TM} \frac{(1+i)^{n_{years}} i}{(1+i)^{n_{years}} - 1} \quad (26)$$

CAPEX definition intrinsically requires the adoption of a straight-line depreciation method. This choice commonly adopted in literature should be regarded as conservative as other deprecation methods would provide higher depreciation rates during the first years thus resulting into a better profitability of the economic analysis.

Operating Costs

The operating costs take into account maintenance and labor costs, personnel costs, chemicals costs, thermal and electric energy costs. The maintenance cost is estimated as the 3% of the CAPEX (on an annual basis), while the labor cost for maintenance is defined as the 20% of the personnel cost [57]. This last term is given by the average cost of the personnel multiplied by the number of required workers, estimated according to [57]. The chemicals cost is given by the sum of the costs relevant to the required pretreatment to apply to the feed (e.g. antiscalant or antifoaming) and to the cooling water (e.g. chlorination) and the post-treatment to the distillate (e.g. chlorination) [57]. The electric energy cost is calculated multiplying the specific electric consumption (assumed equal to 1.5 kWh_{el}/m^3 [64]) by the specific electric energy cost [US$/$kWh_{el}$]. Finally, the thermal energy cost is given by the product of the

required thermal energy (i.e. the required steam times its latent heat) and the specific heat cost, which depends on the source of the heat which is available. In the case of no waste heat available, the heat is supposed to come from a gas turbine co-generation system and its price is function of the required steam pressure and is calculated via the Reference Cycle Method [64] reported in the Supplementary Material section. If waste heat is supposed to be available in the industrial site, a certain cost for the thermal energy is given, depending on its quality. This cost is different from zero to account for the cost of the infrastructures necessary to supply the steam and, for the case of a higher-pressure steam, since this does not constitute a waste stream, a purchase price has been estimated on the bases of industrial practical data. In the case under investigation, part of the feed itself is employed as the cooler in the end condenser, so this cost has not to be accounted among the operating costs. The total annual operating cost (OPEX in US$/y) is given by the sum of all the described operating cost terms.

Levelized Brine Cost

The capital and the operating costs can be estimated also per unit of valuable solution produced, being expressed in this case in US$/m^3. As reported by Papapetrou et al. [60], in order to compare the feasibility of different desalination technologies, the levelized cost of water (LCOW) is commonly used, i.e. the selling price that the water would have to reach the break-even point after a certain plant lifetime. In formula:

$$LCOW = \frac{C_{T_M} + \sum_{t=1}^{n_{years}} \frac{OPEX(t)}{(1+i)^t}}{\sum_{t=1}^{n_{years}} \frac{M_{dist}(t)}{(1+i)^t}} \quad (27)$$

In most of the cases, the LCOW is calculated under the assumption that the produced water flow rate (M_{dist}) and the operating costs are the same for every year in the plant lifetime, thus the definition of the LCOW is as follows.

$$LCOW = \frac{CAPEX + OPEX}{M_{dist}} \quad (28)$$

Literature reports many examples of techno-economic analysis of processes producing water where the Levelized Water Cost is the only profitability index commonly adopted. The MED process investigated in the present work is meant as a unit able to produce a concentrated brine as main product to be sold. Thus, an evaluation standard akin to the LCOW was proposed, namely the Levelized Brine Cost (LBC), as reported in Equation (29):

$$LBC = \frac{CAPEX + OPEX - REVENUE}{M_{brine}} \quad (29)$$

where M_{brine} is the brine flow rate produced by MED in one year [m^3/y]. Notably, the investigated MED unit produces also distillate being a by-product which can be sold. Relevant revenues must be subtracted to the expenses as reported in equation (29). Throughout the work, the definition in Equation (29) corresponds to the total Levelized Brine Cost LBC_{tot}, given by the sum of the Levelized Brine Cost relevant to the CAPEX (LBC_{CAP}) and the Levelized Brine Cost relevant to the OPEX (LBC_{OP}).

3. Description of the Case Study: Treatment of the IEX Effluent

The present work focuses on the investigation of the MED performances within the treatment of the effluent produced by the regeneration process of the Ion Exchange Resins employed in a water softening plant. The results are collected under two assumptions: (i) the effluent does not present organics or other pollutants (such as nitrate or boron) in an appreciable quantity, (ii) the stage of nanofiltration and crystallization ensures the total separation of the bivalent cations. The solution which is fed to the MED presents NaCl and water only and this allows considering a wide range of steam temperatures in the first effect. Two scenarios are investigated: (i) in the first one, all the steam is supposed to be supplied by an external source and, in particular, a gas turbine co-generation system, which is also the source of the electric energy; (ii) in the second one, waste heat is available in the industrial site at certain conditions and at a certain cost, namely either at 1 bar and a cost of 10 US$/$MWh_{th}$ or at 5 bar and a very conservative cost of 30 US$/$MWh_{th}$ [53], [54]. Details are reported in Table 4.

Table 4. Summary of the investigated scenarios.

			T_s	P_m	Heat cost
Scenario 1 (section 4.1)	Case 1	Plane MED	Variable (65-120°C)	$P_{sat,steam}(T_s)$	Variable with P_m, see Eq. (30)
	Case 2	MED-TVC	70°C	Variable (3-21 bar)	Variable with P_m, see Eq. (30)
Scenario 2 (section 4.2)	Case 1	Plane MED	100°C	$P_{sat,steam}(T_s)$ 1 bar	10 US$/$MWh_{th}$ (section 4.2.1.1) Variable (section 4.2.2)
	Case 2	Plane MED	120°C	$P_{sat,steam}(T_s)$	30 US$/$MWh_{th}$ (section 4.2.1.2) Variable (section 4.2.2)
		MED-TVC	70°C	5 bar	30 US$/$MWh_{th}$ (section 4.2.1.2) Variable (section 4.2.2)

In both scenarios, the concentration of the feed is given by the average salinity of the effluent produced during the regeneration of the resins (an overall salinity of around 36,000 ppm, including around 11,000 ppm of NaCl). Usually, this salinity is quite low because of a strong dilution, carried out in the last stages of the regeneration cycle via softened water, in order to flash out completely the spent regenerant from the resins. The concentration of the brine, which has to be produced by the MED plant, is set equal to the required regenerant concentration (90,000 ppm), thus a concentration factor of almost 9 has to be guaranteed by the MED evaporator. All simulations are performed varying the number of effects, both for the plane MED and the MED-TVC system, always with a forward-feed arrangement. In the first scenario, the temperature of the steam supplied to the plane MED varies from 65°C up to 120°C [55], [62]. Conversely, concerning the MED-TVC, the temperature of the steam is fixed equal to 70°C, in order to ensure a stable behavior of the thermo-vapor compressor (C_R < 6) [56], while the pressure of the motive steam is let free to vary from 3 bar up to 21 bar. In the second scenario, the temperature of the steam in the plane MED is selected as the highest temperature possible (≤ 120°C), depending on the quality of the waste heat. Regarding the MED-TVC, its performances are investigated only for the higher-pressure waste heat and the pressure of the motive steam is equal to the pressure of the available waste heat, while the Top Brine Temperature is fixed equal to 70°C. Finally, in both scenarios, the temperature of the last effect is equal to 38°C, in order to ensure a minimum terminal temperature difference of 3°C in the case of the maximum temperature change in the end condenser (10°C). The main technical assumptions are reported in Table 5.

Table 5. Technical inputs for the case study analysis.

Main technical parameters		
X_{feed} [ppm]	11,000	
X_{brine} [ppm]	90,000	
N [-]	variable	
T_s [°C]	variable (MED)	70 (MED-TVC)
P_m [bar]	$P_{sat}(T_s)$ (MED)	variable (MED-TVC)
T_n [°C]	38	
T_{feed} [°C]	25	
M_{feed} [kg/s]	200	

Regarding the economic parameters, the thermal energy cost depends on the pressure of the steam in the first scenario and on the quality of the waste heat in the second scenario. All other parameters are fixed. The electric energy cost is calculated for the electricity produced by a gas turbine co-generation system, the water price is equal to an average distillate price produced in a desalination plant [57]. Since the water price is kept constant in the two scenarios and the produced distillate flow rate is always the same (because the feed flow rate as well as the salinity of the feed and of the brine have been defined), the water revenue is the same in all cases and it is equal to 8.15 $\$/m^3_{brine}$. The depreciation period, the average personal cost and the number of workers are also typical of commercial-scale desalination plants [57], [60], [64]. These parameters are reported in Table 6. It is worth noting that many cost items reported in Table 6 may change significantly when different countries are investigated. Among the cost items, unitary personnel cost of 50,000 US$/y should be regarded again as a conservative choice. Nevertheless, preliminary analysis showed that even doubling this cost, the corresponding LBC remains competitive compared to the fresh regenerant solution cost.

Table 6. Main economic inputs for the case study analysis.

Main economic parameters	
Thermal energy cost	variable
Electric energy cost	0.215 US$/kWh$_{el}$
Discount rate (i)	6%
Depreciation period (n_{years})	25 years
Average unitary personnel cost	50,000 US$/y
Number of workers	10
Pure water price	1US$/m^3
Fuel cost (gas)	65.9 US$/MWh$^{(*)}$

$^{(*)}$ See Supplementary Material section.

Regarding the first scenario, the steam is assumed to be completely supplied by a combined cycle CHP system, fired by natural gas, and its cost is reported as a function of the steam pressure P_m in Figure 4. The costs are calculated via the application of the Reference Cycle

Method [64], described in the Supplementary materials. It is evident that the heat cost increases more deeply in the range of pressure between 0 and 1 bar; conversely, for pressures higher than 1 bar the increasing trend is smoother. The trend of the cost vs. the pressure of the steam is fitted via a logarithmic equation, as reported in Equation (30), which is valid for the natural gas cost shown in Table 6.

$$Heat\ cost\ \left[{}^{US\$}/_{MWh_{th}}\right] = 10.7 \ln P_{steam} + 24.2 \qquad (30)$$

This has important consequences in the estimation of the operating costs of both MED and MED-TVC in the first scenario. In fact, the temperature of the total steam to supply to the plane MED ranges from 65°C to 120°C and, consequently, its pressure ranges from 0.25 bar to 1.98 bar. Conversely, the pressure of the motive steam, which can be supplied to the TVC, in the case of the MED-TVC system, can vary from 3 bar up to 21 bar, as it is defined as the maximum pressure of the steam produced by the co-generation system.

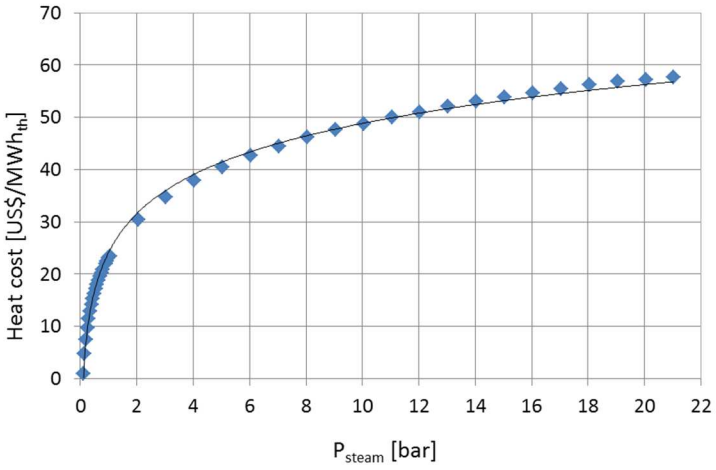

Figure 4. Thermal energy cost vs. the steam pressure for the case of a gas turbine co-generation system. (as a reference, the pressures of 1, 5, 10, 15 and 20 bar correspond to temperatures of 99.7, 151.9, 179.9, 198.2, 212.2°C)

Finally, as already mentioned, the feasibility of the MED technology is evaluated comparing the calculated LBC_{tot} with the current cost of the regenerant solution, equal to 8 US$/m^3. This cost is estimated for a 9%$^{w/w}$ NaCl-water solution, considering a cost of the pure NaCl salt equal to 65 euro/ton (80.2 US$/ton) and a cost of water equal to 1 US$/m^3. Notably, a preliminary analysis on the treatment chain of Figure 1 showed that the revenues deriving from the selling of $Ca(OH)_2$ and $Mg(OH)_2$ more than counterbalance all the costs relevant to the crystallization and filtration steps [58]. Thus, the value of 8 US$/m^3 of the current regenerant solution is used as a benchmark for the MED technology only.

4. Results and Discussion

4.1 First scenario: steam supplied by a gas turbine co-generation system

In the first scenario, the influence of T_s in the plane MED and of P_m in the MED-TVC is evaluated at 6, 9, 12 and 15 effects. Figure 5 reports the trend of the total Levelized Brine Cost (LBC_{tot} in US\$/m^3), considering the contributions of the capital (LBC_{CAP}) and the operating costs (LBC_{OP}) for a plane MED with different number of effects varying the steam temperature. The (threshold) purchase cost of fresh regenerant solution is also reported for comparison purposes. Basically, the capital costs slightly decrease with T_s because of the higher overall temperature differences, which correspond to higher available driving forces in each effect. Therefore, whenever the available temperature driving force increases, the area required for the heat transfer decreases. Conversely, the operating costs increase very sharply, because of the higher thermal energy cost. The analysis at different number of effects highlights the different weights of the capital and the operating costs in the different configurations, i.e. the higher the number of effects, the higher the impact of the fixed costs on the total LBC compared to the operating costs. Therefore, at 6 and 9 effects, the operating costs are higher than the capital costs in most of the range of T_s. Conversely, at 12 and especially at 15 effects, the two cost terms are comparable and, although the LBC_{tot} increases also in these two cases in the entire range of T_s, it is possible to notice a low-slope trend at low temperatures, because the capital and operating cost trends are opposite. Finally, it is also worth mentioning that, especially for high number of effects, for any temperature lower than 80°C, the total LBC is lower than the current cost of the regenerant solution (i.e. 8 US\$/m^3).

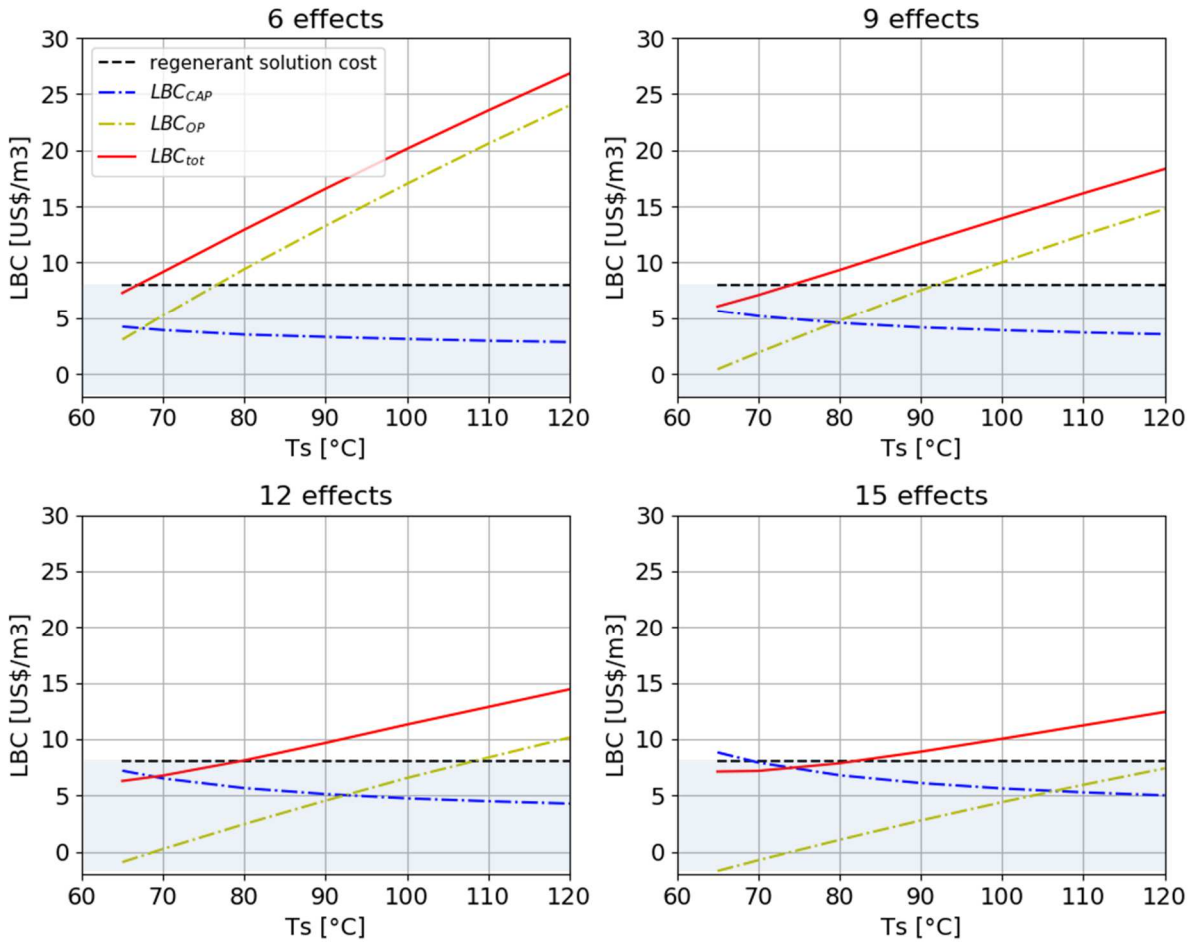

Figure 5. Levelized Brine Cost for a plane MED system with variable number of effects (6, 9, 12, 15 effects) as a function of the steam temperature.

Conversely, Figure 6 shows the trend of the LBC_{tot}, together with the LBC_{CAP}, LBC_{OP} and the regenerant solution cost for a MED-TVC system with different number of effects, varying the motive steam pressure. In this case, as already mentioned, T_s is fixed and equal to 70°C and this leads to constant capital costs. Conversely, P_m is free to vary and its variation leads to a variation of the operating costs. The slope is higher at low P_m and decreases at higher pressures in accordance with Figure 4. Overall, comparing the results at different number of effects, as expected, the capital costs increase as the number of effects increases, while the operating costs strongly decrease. Note that, in this case, at 6 and 9 effects the operating costs are always higher than the capital costs, at 12 effects there is a cross at low pressures, while at 15 effects the capital costs are always higher that the operating costs. Finally, for the MED-TVC system, the cost of the thermal energy is too high to make this system competitive with the current regenerant solution supply. In fact, for any configuration and for any pressure in the investigated range, the LBC_{tot} is higher than the estimated cost of the required regenerant solution of 8 US$/m^3.

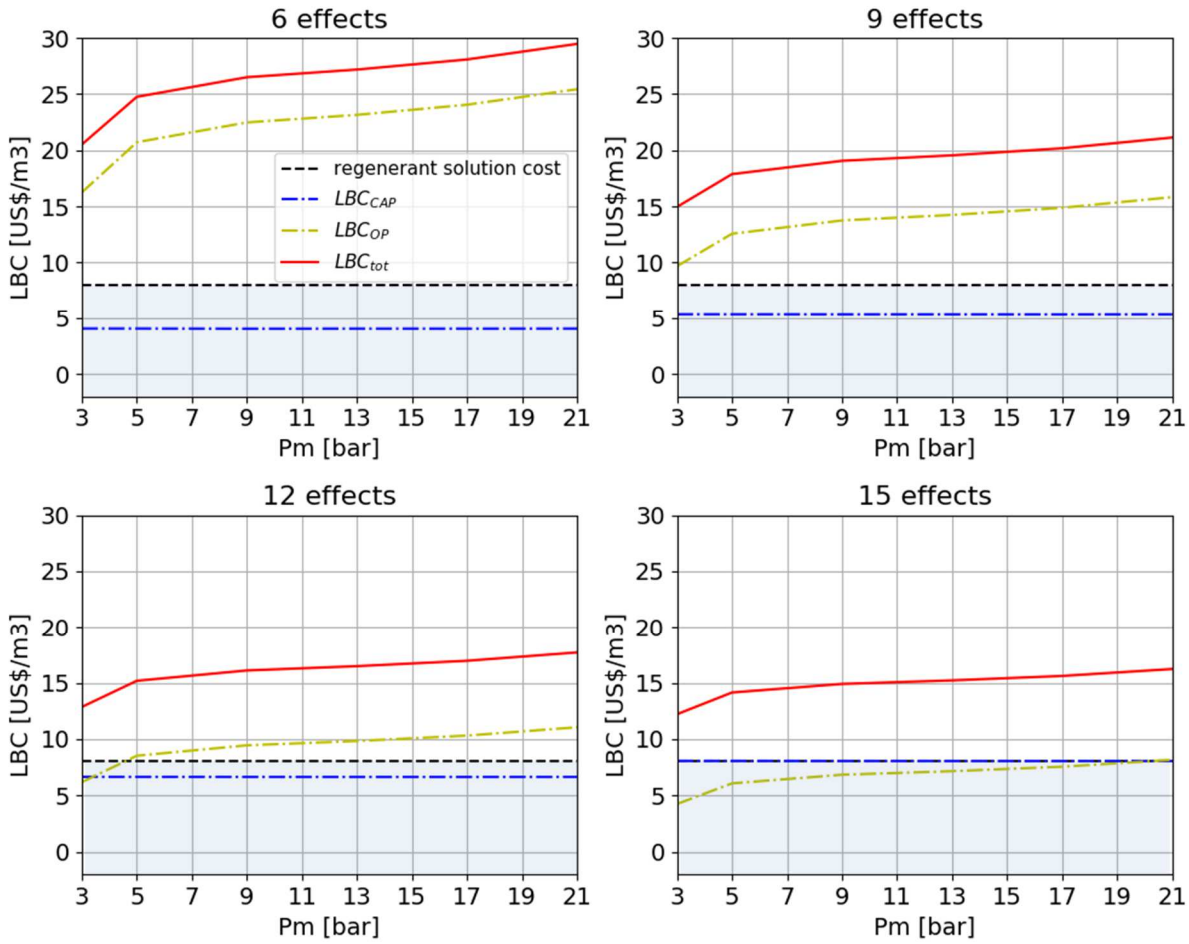

Figure 6. Levelized Brine Cost for a MED-TVC system with variable number of effects (6, 9, 12, 15 effects) as a function of the motive steam pressure.

4.2 Second scenario: waste heat available in the industrial site

4.2.1 *Fixed revenue and operating costs*

In the second scenario, the thermal energy is assumed to be supplied via waste heat, available in the industrial site. In particular, two sets of thermo-physical conditions of the available steam (i.e. temperature and pressure) are selected and coupled with a value of the thermal energy cost: saturated steam at 1 bar at a cost of 10 US$/MWh$_{th}$ and saturated steam at 5 bar and a cost of 30 US$/MWh$_{th}$ (see Table 4). In the first case, only the plane MED is investigated, since the pressure is too low for a MED-TVC (typically P_m > 3bar [59]). For the second accounted waste heat quality, the plane MED and the MED-TVC systems are both investigated and a sensitivity analysis varying the number of effects is performed. For the MED-TVC system, the pressure of the motive steam is equal to the pressure of the available steam (5 bar). Conversely, for the plane MED, the temperature of the steam in the first effect is set equal to the maximum reachable temperature of the steam, taking into account the steam pressure and the maximum allowed temperature in the first effect (i.e. 120°C). This is because

the higher the temperature of the steam, the lower the fixed costs, which are the most relevant costs for the definition of the LBC_{tot}, when the thermal energy cost is fixed.

4.2.1.1 First case: waste heat available at 1 bar

In Figure 7 the trends of the LBC_{CAP}, LBC_{OP} and LBC_{tot} are reported as functions of the number of effects. As expected, the capital costs increase with the number of effects, while the operating costs decrease. The combination of these two opposite trends gives rise to a minimum in LBC_{tot}, which occurs at 13 effects. Interestingly, for any number of effects higher than 5, LBC_{tot} results lower than 8 US$/m^3, showing that, in these conditions, the technology is competitive with the current regenerant solution supply. In particular, the minimum LBC_{tot} is around 4 US$/m^3.

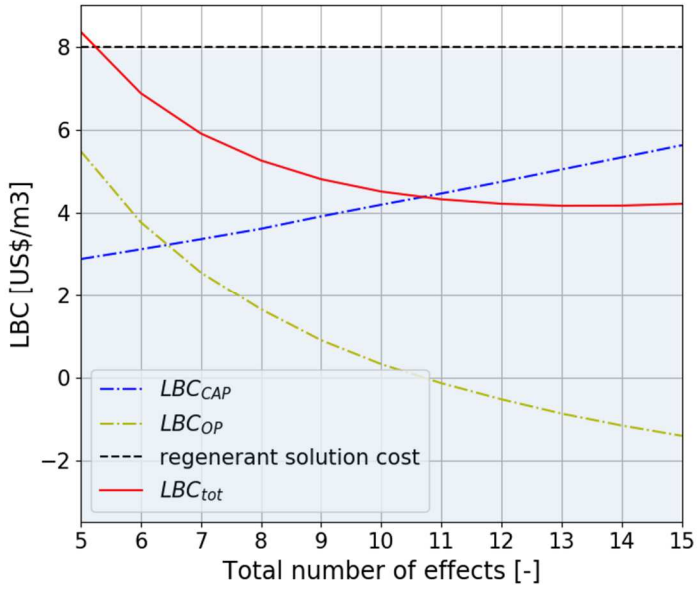

Figure 7. Levelized Brine Cost for a plane MED system with T_s = 100°C varying the number of effects (5-15 effects) and fixing the thermal energy cost equal to 10 US$/MWh$_{th}$.

4.2.1.2 Second case: waste heat available at 5 bar

The results relevant to this case are reported in Figure 8. Both in the case of the plane MED and of the MED-TVC, the operating costs play the most prominent role in the definition of LBC_{tot} and, for this reason, a wider range of number of effects has to be investigated to detect the minimum. The minimum corresponds to the optimum configuration of the system, and it is found at different number of effects because of the different weights of the capital and the operating costs in the plane MED and in the MED-TVC. The capital costs are higher in the MED-TVC in the entire range of number of effects, because of the presence of the TVC but, mainly, because of the lower available driving force, due to the fixed T_s = 70°C. At the same time, the operating costs are much higher in the plane MED, especially at low number of

effects, because the total steam, which has to be supplied, is higher than the motive steam supplied at the same cost in the MED-TVC. In both cases (MED and MED-TVC) it is possible to recognize a minimum in LBC_{tot}, which occurs at 25 effects for the plane MED and at 15 effects for the MED-TVC. These two LBC_{tot} minimum values are around 10 US$/m^3, which is higher than the current cost of the fresh regenerant solution. This means that the employment of this waste heat stream does not make this technology competitive with the current state.

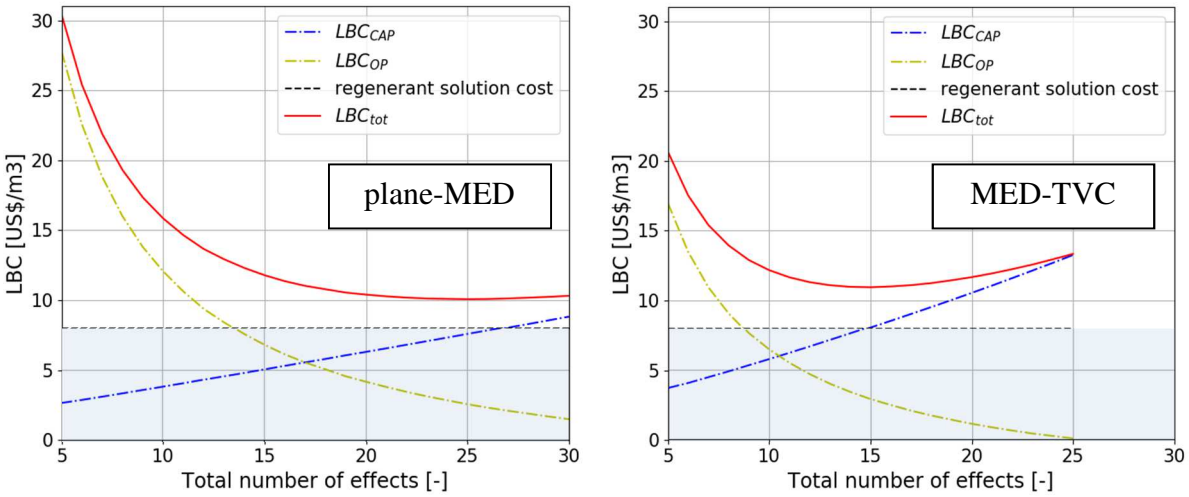

Figure 8. Levelized Brine Cost for a plane MED system (left) with T_s = 120°C and for a MED-TVC system (right) with P_m = 5bar varying the number of effects and fixing the thermal energy cost equal to 30 US$/MWh$_{th}$.

4.2.2 *Sensitivity analysis*

A sensitivity analysis is carried out varying the thermal energy cost from 0 [60] up to the cost of the steam (see Figure 4) produced by the co-generation system at the corresponding pressure (1bar for the first case in Figure 7 and 5 bar for the second case in Figure 8). This analysis aims at investigating quantitatively the role of the thermal energy cost on the LBC_{tot} and at defining the optimum system configuration (i.e. the number of effects, for plane MED and MED-TVC), for the two different steam qualities of Case 1 and Case 2. Figure 9 reports the minimum LBC_{tot} varying the thermal energy cost from 0 up to the selling price at 1 bar (i.e. 26 US$/MWh$_{th}$ from Figure 4), for the plane MED described in the Case 1 of the second scenario. The chart shows an increasing trend of the minimum LBC_{tot} with the thermal energy cost, as expected. Moreover, the number of effects corresponding to the optimum configuration increases with the thermal energy cost. Therefore, since the heat cost increases, the operating costs constitute a larger fraction of the total costs and the optimum system configuration corresponds to a higher number of effects and a lower thermal consumption.

Finally, it is remarkable that at very low heat cost, the minimum LBC_{tot} is negative and this means that the revenue coming from the water production overcomes the annualized capital and operating costs.

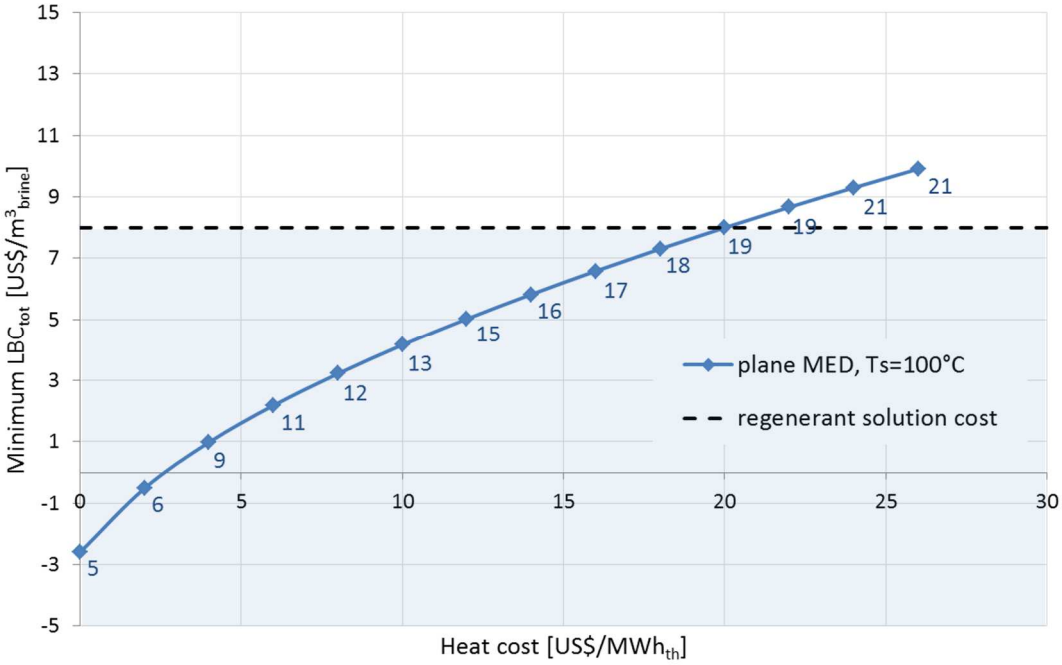

Figure 9. Minimum LBC_{tot} as a function of the heat cost [US$/$MWh_{th}$] for a plane MED (steam at P=1 bar, T_s=100°C). The labels correspond to the number of effects, which minimizes LBC_{tot}.

Figure 10 reports the trends of the minimum LBC_{tot} for the plane MED and the MED-TVC described in Case 2 of the second scenario. Here, the optimum number of effects ranges up to 30 effects for the plane MED and up to 17 effects for the MED-TVC, because of the higher maximum thermal energy cost (i.e. 42 US$/$MWh_{th}$ at P_m = 5bar, see Figure 4). It is worth noting that, in the entire range of heat cost, the plane MED system ensures the lowest minimum LBC_{tot}, but employing always a higher number of effects, for a given heat cost. Moreover, it is possible to notice that the higher the heat cost, the larger the difference between the optimum configurations in the two systems. The plane MED has higher thermal consumptions on the one hand. On the other hand, it allows a larger reduction of operating costs, increasing the number of effects, with respect to the MED-TVC. Therefore, the capital costs increase much more deeply with the number of effects in the MED-TVC, because of the stronger depletion of the driving force, due to the lower steam temperature (70°C). This leads to a higher value of the minimum LBC_{tot} with respect to the plane MED. It is also possible to notice that the trends relevant to the two configurations starts at 0 with a certain difference, they get closer at low heat costs and start diverging at higher heat costs. For a heat cost equal

to 0, the CAPEX is the prominent term and it is lower for the plane MED, because of the higher T_s. As the heat cost increases, the OPEX acquires a more significant role and the minimum LBC_{tot} values get similar. At very high heat cost, both systems tend to a configuration, which minimizes the operating costs increasing the number of effects and at this point the capital costs are the prominent term in the calculation of LBC_{tot}. This explains why the plane MED is the most competitive arrangement, especially at high thermal energy costs. Finally, when comparing the minimum LBC_{tot} for the plane MED at the two different T_s (i.e. 100°C in Figure 9 and 120°C in Figure 10), similar results can be observed. This is not surprising since the values correspond to the minimum costs and the optimum configuration (i.e. the optimum number of effects) takes into account the different operating conditions. Therefore, the optimum number of effects for the plane MED is always lower (or equal for very low heat cost) for the case of T_s = 100°C, which allows having a higher temperature difference in each effect. Finally, it is worth noting that, in both cases, at a heat cost of around 20 US$/MWh$_{th}$, the minimum LBC_{tot} reaches a value of 8 US$/m^3, which is the current cost of the fresh regenerant solution. This means that the competitiveness of the process presented in the present work with respect to the traditional one is achieved when heat cost is lower than the threshold value of 20 US$/MWh$_{th}$.

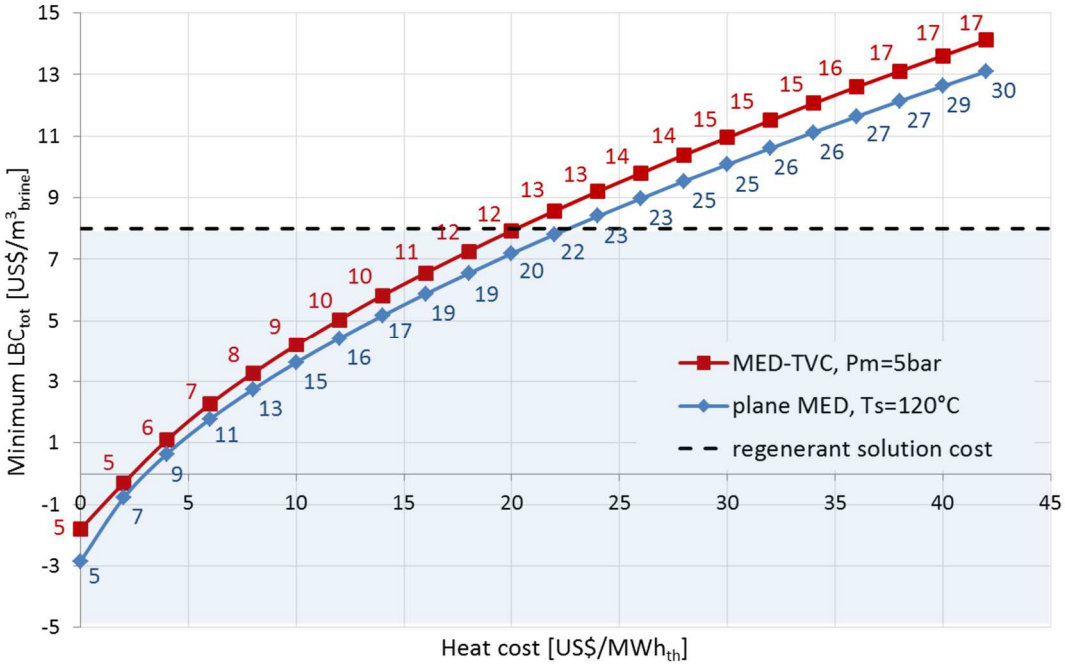

Figure 10. Minimum LBC_{tot} as a function of the heat cost [US$/MWh$_{th}$] for a plane MED ($T_s$=120°C) and for a MED-TVC (P_m=5bar). The labels correspond to the number of effects which minimize LBC_{tot}.

Finally, for both Case 1 and Case 2 a parametric analysis is performed taking as a reference the configuration which minimizes LBC_{tot} and varying independently the main operating costs, i.e. electric energy cost, thermal energy cost and the water selling price, in a range within -100% and +100% of the corresponding costs in the reference case. The energy cost and the water price variations are not related to a variation in the quality of the supplied energy (e.g. the steam temperature) or of the produced water (since the distillate produced by the MED plant is supposed to be pure water in all cases). The analyses aim at investigating how much the single costs influence the overall LBC and which are the ranges of costs and prices that ensure the economic feasibility of the plant. These analyses are reported in Figure 11 and in Figure 12. Figure 11 is relevant to Case 1, i.e. a plane MED with T_s = 100°C and N = 13. In the reference case, the thermal energy cost is fixed equal to 10 US$/kWh$_{th}$. It is evident that the water selling price has the highest impact on LBC_{tot}, since its 100% variation leads to an opposite variation of LBC_{tot} of about 200%. The second term for relevance is the thermal energy cost, followed by the electric energy cost, as expected since the thermal energy is the main energy form required. Note that the percentage variation of LBC_{tot}, which corresponds to the current price of the salt solution (i.e. 8 US$/m^3) is also observable in Figure 11 and in Figure 12 . One can observe that for the whole range of variation of the electric energy cost, the LBC_{tot} keeps lower than the threshold value, while a maximum increase of 80% of the thermal energy cost or a maximum decrease of around 50% of the water selling price could still ensure the competitiveness of the technology.

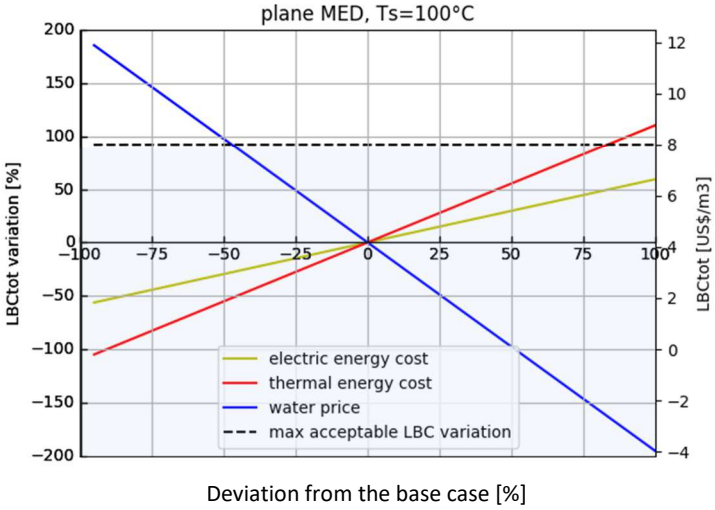

Figure 11. Parametric analysis of the LBC_{tot} of a plane MED varying the main operating costs (thermal energy cost, electric energy cost and water selling price) with respect to the reference case: thermal energy cost = 10 US$/MWh$_{th}$, electric energy cost = 0.215 $/kWh$_{el}$, water price = 1 US$/m^3, N = 13.

Conversely, the two charts in Figure 12 are relevant to Case 2, i.e. for the plane MED T_s = 120°C and N = 25, while for the MED-TVC P_m = 5 bar and N = 15. As it can be seen, the dependence of LBC_{tot} on the operating costs variation is much weaker than in the previous case, because these configurations are characterized by the prominence of the capital costs, as already mentioned. As a difference from Case 1, here the water selling price and the thermal energy cost have a comparable, yet opposite, role. Conversely, also in this case, the variation of the electric energy cost has a slight impact compared to the other two. Note that the variation of the minimum LBC_{tot} leading to LBC_{tot} equal to the current regeneration solution cost is negative, since in both cases the minimum LBC_{tot} is higher than 8 US$/m^3, even for the optimum configuration. In particular, a water selling price increase or a thermal energy cost decrease of the same amount, which is 25% for MED and around 30% for MED-TVC could make the technology competitive with the current purchase of fresh regenerant solution. Finally, in this last case, the charts for the plane MED and for the MED-TVC are almost identical, because in both systems the steam requirement was minimized by increasing the number of effects, in order to limit the role of the heat cost as much as possible.

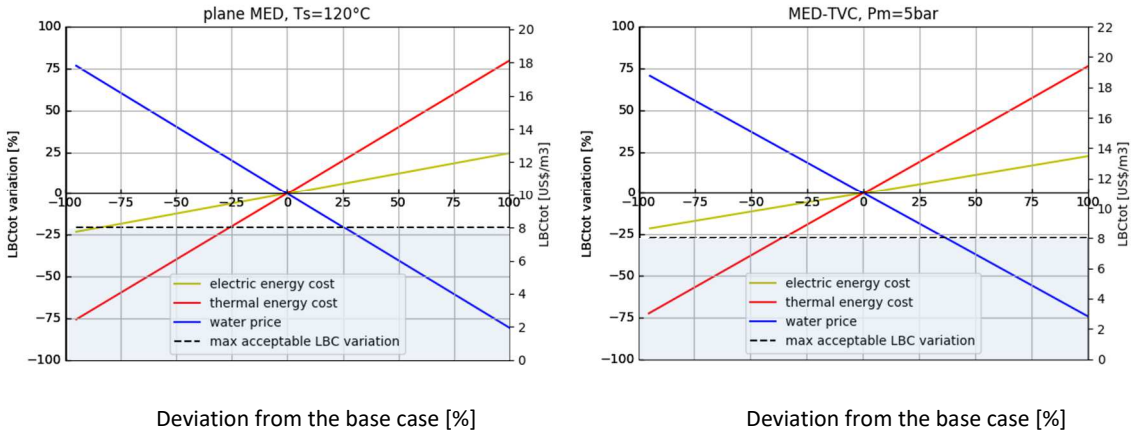

Figure 12. Parametric analysis of the LBC_{tot} for plane MED (left) and for MED-TVC (right) varying the main operating costs (thermal energy cost, electric energy cost and water selling price) with respect to the reference case: thermal energy cost = 30 US$/MWh$_{th}$, electric energy cost = 0.215 $/kWh$_{el}$, water price = 1 US$/m^3, N_{MED} = 25, $N_{MED\text{-}TVC}$ = 15.

The analyses reported in Results and Discussion section are relevant to a certain size of the plant. In order to evaluate how much the size affects the overall costs, a sensitivity analysis is performed varying the feed flow rate, which determines the plant design and the relevant economic assessment. With this regard, the results given by the module costing technique adopted are compared with the results of another method (here referred as Gebel method) proposed in literature for thermal desalination plants [61], [64]. As shown in Figure 13, LBC_{tot} shows a decreasing trend as M_{feed} increases, as expected due to economy of scale. It is

also remarkable that the two correlations show a very good agreement in the range of flow rates higher than 100 kg/s, while the values diverge at lower flow rates. This occurs because the present method intrinsically account for equipment size, thus being suitable also for very low scales (e.g. the correlation for the heat exchangers is valid down to a heat exchanger area equal to 10 m^2). Conversely, the Gebel method was developed for desalination plants of higher scale and, for this reason, the costs are allegedly underestimated at smaller scales.

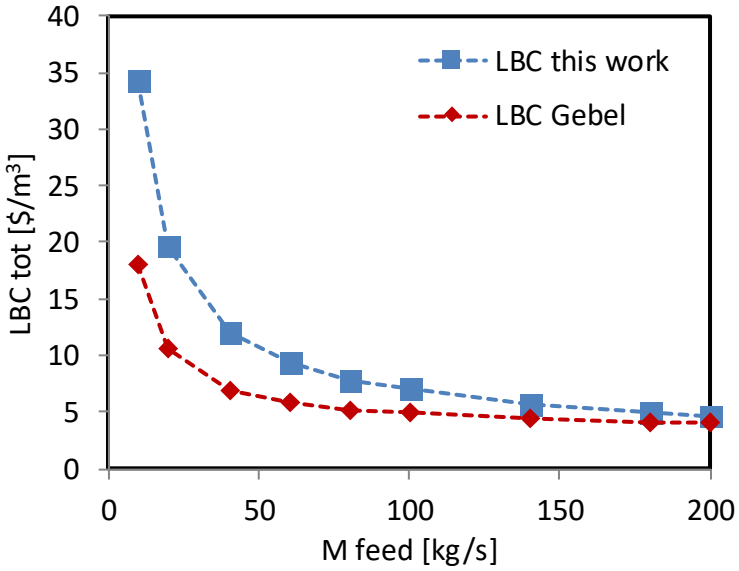

Figure 13. Sensitivity analysis of the LBCtot as function of the feed flow rate (Mfeed [kg/s]) for the reference case 1: thermal energy cost = 10 US$/$MWh_{th}$, electric energy cost = 0.215 $/$kWh_{el}$, water price = 1 US$/m^3, N = 13.

5. Conclusions

In the present work, the feasibility to apply the Multi-Effect Distillation technology to the treatment of the IEX spent regenerant solution was investigated via a techno-economic analysis. The treatment aims at the recycling of the solution through a purification and a re-concentration stage. The re-concentration occurs in the MED plant, which has to concentrate the solution from 11,000 ppm up to 90,000 ppm. Because of this wide concentration range, the forward-feed arrangement was selected and the performances of a plane MED were compared with those of a MED-TVC system. An integrated techno-economic model was developed in order to assess the present process feasibility. To this aim, a novel performance indicator, named the total Levelized Brine Cost (LBC_{tot}), was proposed and provided as output by the model. This value, given by the combination of the capital and the operating costs and the revenue coming from the selling of the produced pure water, was compared with the current cost of the fresh regenerant solution (i.e. 8 US$/$m^3$). Two scenarios were

investigated: in the first one, the steam was assumed to be supplied by a gas turbine co-generation system and its cost was a function of the pressure. In this scenario, the temperature of the steam in the plane MED and the pressure of the motive steam in the MED-TVC were varied, at different number of effects. The results showed that producing the regenerant solution with the plane MED with high number of effects (> 12) and low T_s (< 80-90°C) costs less than buying a fresh regenerant solution. This is not the case for all the analysis performed with the MED-TVC. The second scenario concerned the availability of waste heat, to be employed as the heating steam. Two different waste heat qualities and costs were tested: saturated steam at 1 bar and 10 US$/MWh$_{th}$ and saturated steam at 5 bar and 30 US$/MWh$_{th}$. Firstly, a sensitivity analysis varying the number of effects was performed for a plane MED and a MED-TVC (only in the case of higher-pressure waste steam). In the first case, the plane MED showed the lowest LBC_{tot} of around 4 US$/m^3 at 13 effects. Conversely, in the second case, the prominence of the thermal energy cost determined a net increase of the LBC_{tot} both for the MED and the MED-TVC and the lowest LBC_{tot} was relevant to a MED system with 25 effects and equal to around 10 US$/m^3. This means that only the employment of the waste heat at 1 bar and 10 US$/MWh$_{th}$ may allow the MED technology to be more convenient than the employment of fresh regenerant.

Moreover, a sensitivity analysis varying the thermal energy cost was performed, in order to evaluate the optimum number of effects (i.e. those that minimize the LBC_{tot}) at the different costs. It resulted that the plane MED reported always a lower LBC_{tot} with higher optimum number of effects in comparison to the MED-TVC. More important, the thermal energy cost of 20 US$/MWh$_{th}$ was identified as the threshold cost value below which the MED technology is economically more advantageous.

Finally, taking into account the optimum configuration (i.e. the optimum number of effects) in the two different cases, for the plane MED and the MED-TVC, a sensitivity analysis varying the thermal energy cost, the electric energy cost and the water selling price was carried out. In the case of the waste steam at lower pressure (first case), the pure water selling price had the highest impact in the definition of LBC_{tot}. Conversely, in the case of the higher waste steam pressure (second case), the water selling price and the thermal energy cost had a comparable role, but it should be pointed out that the overall impact of the operating cost was lower, because the optimum configuration was meant to minimize the operating costs, increasing the number of effects.

Overall, the present study results suggest that applying the MED technology instead of supplying fresh NaCl solution in every regeneration cycle may result not only into a net

reduction of raw material consumption and of environmental pollution, but also into a cost saving in a wide range of conditions (both technical and economical). The next steps will address the economic optimization of the whole treatment chain reported in Figure 1, taking into account the use of different reactants, operating conditions and different unit configurations (e.g. different crystallizers). The outcome of this analysis should boost future and more in-depth analysis of other treatment processes involving the production of saline solutions, also in other industrial sectors, such as the textile or the mining industry, aiming at increasing the level of sustainability of the industrial processes.

Acknowledgements

This work was funded by the ZERO BRINE project (ZERO BRINE – Industrial Desalination – Resource Recovery – Circular Economy) - Horizon 2020 programme, Project Number: 730390: www.zerobrine.eu.

Nomenclature

N	number of effects [-]
M	mass flow rate [kg/s]
T	temperature [°C]
X	salinity [ppm]
P	pressure [bar]
A	heat exchanger area [m^2]
sA	specific area [m^2/(kg/s)]
sQ	specific thermal consumption [kJ/kg]
h	specific enthalpy [kJ/kg]
C_p	specific heat [kJ/(kg °C)]
U	overall heat transfer coefficient [kW/(m^2 °C)]
C_R	compression ratio [-]
ER	expansion ratio [-]
Ra	entrainment ratio [-]
C_{BM}	bare module cost [US$]
C_p^0	purchased cost of equipment [US$]
F_{BM}	bare module factor [-]
F_M	correction factor due to construction materials [-]
F_P	correction factor due to the working pressure [-]
C_{TM}	total module cost [US$]
i	discount rate [-]
n_{years}	depreciation period
CAPEX	annualized capital costs [US$/y]
OPEX	annualized operating costs [US$/y]

Greek letters

λ	latent heat [kJ/kg]
ΔT	temperature difference [°C]
α_{cond}	fraction of vapor condensed in the preheater

Subscripts

feed	feed entering into the first effect
dist	outlet distillate
brine	outlet brine
HX	heat exchanger
preh	preheater
cond	end-condenser
s	total steam
m	motive steam
vap	total vapor generated in the generic effect
d	vapor generated via evaporation
f,brine	vapor generated via the brine flash
fb	vapor generated in the flash box
b	brine solution generated in the generic effect
c	condensed pure water collected in the flash box
cw	cooling water
sw	salt water solution
liq	pure water in the liquid state
vap	pure water in the vapor state
n	last effect index
ev	entrained vapor
_real	fixed distillate flow rate to be produced

Acronyms

IEX	Ion Exchange Resins
MED	Multi-Effect Distillation
TVC	Thermo-vapor compressor
GOR	Gain Output Ratio
FF	Forward Feed
NF	Nanofiltration
RO	Reverse Osmosis
LBC	Levelized Brine Cost [US$/$m^3$]
BPE	Boiling Point Elevation [°C]
DTML	Temperature logarithmic mean

LCOW	Levelized Cost of Water [US$/m^3]
SCOW	Simplified Cost of Water [US$/m^3]
CHP	Combined heat and power

Bibliography

[1] R. Einav, K. Harussi, and D. Perry, "The footprint of the desalination processes on the environment," *Desalination*, vol. 152, pp. 141–154, 2002.

[2] T. Mezher, H. Fath, Z. Abbas, and A. Khaled, "Techno-economic assessment and environmental impacts of desalination technologies," *Desalination*, vol. 266, pp. 263–273, 2011.

[3] T. Bleninger and G. H. Jirka, "Modelling and environmentally sound management of brine discharges from desalination plants," *Desalination*, vol. 221, pp. 585–598, 2008.

[4] A. Giwa, S. Daer, I. Ahmed, P. R. Marpu, and S. W. Hasan, "Experimental investigation and artificial neural networks ANNs modeling of electrically-enhanced membrane bioreactor for wastewater treatment," *Journal of Water Process Engineering*, vol. 11, pp. 88–97, 2016.

[5] J. Morillo, J. Usero, D. Rosado, H. E. Bakouri, A. Riaza, and F. J. Bernaola, "Comparative study of brine management technologies for desalination plants," *Desalination*, vol. 336, pp. 32–49, 2014.

[6] A. Giwa, V. Dufour, F. A. Marzooqi, M. A. Kaabi, and S. W. Hasan, "Brine management methods: Recent innovations and current status," *Desalination*, vol. 407, pp. 1–23, 2017.

[7] A. Pérez-González, A. M. Urtiaga, R. Ibáñez, and I. Ortiz, "State of the art and review on the treatment technologies of water reverse osmosis concentrates," *Water Research*, vol. 46, no. 2, pp. 267–283, 2012.

[8] C. M. Tun and A. M. Groth, "Sustainable integrated membrane contactor process for water reclamation, sodium sulfate salt and energy recovery from industrial effluent," *Desalination*, vol. 283, pp. 187–192, 2011.

[9] M. Turek, P. Dydo, and A. Surma, "Zero discharge utilization of saline waters from 'Wesola' coal-mine," *Desalination*, vol. 185, pp. 275–280, 2005.

[10] S. H. Zyoud, A. E. Al-Rawaifeh, H. Q. Shaheen, and D. Fuchs-Hanusch, "Benchmarking the scientific output of industrial wastewater research in Arab world by utilizing bibliometric techniques," *Environ Sci Pollut Res*, vol. 23, pp. 10288–10300, 2016.

[11] D. Ariono, M. Purwasasmita, and I. G. Wenten, "Brine Effluents: Characteristics, Environmental Impacts and Their Handling," *J. Eng. Technol. Sci.*, vol. 48, no. 4, pp. 367–387, 2016.

[12] E. Drioli, E. Curcio, G. D. Profio, F. Macedonio, and A. Criscuoli, "Integrating Membrane Contactor Technology and Pressure-Driven Membrane Operations for Seawater Desalination Energy, Exergy and Costs Analysis," *Chemical Engineering Research and Design*, vol. 84, pp. 209–220, 2006.

[13] L. Bilińska, M. Gmurek, and S. Ledakowicz, "Textile wastewater treatment by AOPs for brine reuse," *Process Safety and Environmental Protection*, vol. 109, pp. 420–428, 2017.

[14] S. D. Alexandratos, "Ion-Exchange Resins: A Retrospective from Industrial and Engineering Chemistry Research," *Ind. Eng. Chem. Res.*, vol. 48, pp. 388–398, 2009.

[15] W. S. Miller, C. J. Castagna, and A. W. Pieper, "Understanding ion-exchange resins for water treatment systems," *Water Technologies and Solutions*, 1981.

[16] Lenntech, "Ion Exchange Introduction," *www.lenntech.com*, 2008.

[17] S. Wadley, C. J. Brouckaert, L. A. D. Baddock, and C. A. Buckley, "Modelling of nanofiltration applied to the recovery of salt from waste brine at a sugar decolourisation plant," *Journal of Membrane Science*, vol. 102, pp. 163–175, 1995.

[18] A. Kapoor and T. Viraraghavan, "Nitrate Removal from Drinking Water-Review," *Journal of Environmental Engineering*, vol. 123, 1997.

[19] J. P. Van der Hoek and A. Klapwijk, "Reduction of Regeneration Salt Requirement and Waste Disposal in an Ion Exchange Process for Nitrate Removal from Ground Water," *Waste Management*, vol. 9, pp. 203–210, 2008.

[20] S. G. Lehman, M. Badruzzaman, S. Adham, D. J. Roberts, and D. A. Clifford, "Perchlorate and nitrate treatment by ion exchange integrated with biological brine treatment," *Water Research*, vol. 42, no. 4, pp. 969–976, 2008.

[21] J. K. Choe, A. M. Bergquist, S. Jeong, J. S. Guest, C. J. Werth, and T. J. Strathmann, "Performance and life cycle environmental benefits of recycling spent ion exchange brines by catalytic treatment of nitrate," *Water Research*, vol. 80, pp. 267–280, 2015.

[22] M. Kabsch-Korbutowicz, J. Wisniewski, S. Łakomska, and A. Urbanowska, "Application of UF, NF and ED in natural organic matter removal from ion-exchange spent regenerant brine," *Desalination*, vol. 280, pp. 428–431, 2011.

[23] M. Gryta, K. Karakulski, M. Tomaszewska, and A. Morawski, "Treatment of effluents from the regeneration of ion exchangers using the MD process," *Desalination*, vol. 180, pp. 173–180, 2005.

[24] EVIDES INDUSTRIEWATER, "Personal communication."

[25] www.zerobrine.eu, "Zero Brine."

[26] A. M. Hassan, M. A. K. Al-Sofi, A. M. Al-Amoudi, A. T. M. Jamaluddin, A. M. Farooque, A. Rowaili, A. G. I. Dalvi, N. M. Kither, G. M. Mustafa, and I. A. R. Al-Tisan, "A new approach to membrane and

thermal seawater desalination processes using nanofiltration membranes (Part 1)," *Desalination*, vol. 118, pp. 35–51, 1998.
[27] A. A. Al-Hajouri, A. S. Al-Amoudi, and A. M. Farooque, "Long term experience in the operation of nanofiltration pretreatment unit for seawater desalination at SWCC SWRO plant," *Desalination and Water Treatment*, vol. 51, no. 7–9, pp. 1861–1873, 2013.
[28] W. L. Ang, A. W. Mohammad, N. Hilal, and C. P. Leo, "A review on the applicability of integrated/hybrid membrane processes in water treatment and desalination plants," *Desalination*, vol. 363, pp. 2–18, 2015.
[29] E. Drioli, F. Lagana, A. Criscuoli, and G. Barbieri, "Integrated membrane operations in desalination processes," *Desalination*, vol. 122, pp. 141–145, 1999.
[30] A. E. Al-Rawajfeh, "Influence of Nanofiltration Pretreatment on Scale Deposition in Multi-stage Flash Thermal Desalination Plants," *Thermal Science*, vol. 15, no. 1, pp. 55–65, 2011.
[31] A. E. Al-Rawaifeh, H. E. S. Fath, and A. A. Mabrouk, "Integrated Salts Precipitation and Nano-Filtration as Pretreatment of Multistage Flash Desalination System," *Heat Transfer Engineering*, vol. 33, pp. 272–279, 2011.
[32] A. E. Al-Rawajfeh, "Nanofiltration pretreatment as CO2 deaerator of desalination feed: CO2 release reduction in MSF distillers," *Desalination*, vol. 380, pp. 12–17, 2016.
[33] A. E. Al-Rawajfeh, H. Glade, and J. Ulrich, "Scaling in multiple-effect distillers: the role of CO2 release," *Desalination*, vol. 182, pp. 209–219, 2005.
[34] Y. M. El-Sayed and R. S. Silver, *Principles of Desalination*. K. S. Spiegler and A. D. K. Laird, 1980.
[35] R. K. Kamali, A. Abbassi, and S. A. S. Vanini, "A simulation model and parametric study of MED–TVC process," *Desalination*, vol. 235, pp. 340–351, 2009.
[36] R. K. Kamali, A. Abbassi, S. A. Sadough Vanini, and M. S. Avval, "Thermodynamic design and parametric study of MED-TVC," *Desalination*, vol. 222, pp. 596–604, 2008.
[37] A. O. Bin Amer, "Development and optimization of ME-TVC desalination system," *Desalination*, vol. 249, pp. 1315–1331, 2009.
[38] K. H. Mistry, M. A. Antar, and V. J. H. Lienhard, "An improved model for multiple effect distillation," *Desalination and Water Treatment*, vol. 51, pp. 807–821, 2013.
[39] H. Sayyadi and A. Saffari, "Thermoeconomic optimization of multi effect distillation desalination systems," *Applied Energy*, vol. 87, pp. 1122–1133, 2010.
[40] H. Sayyadi, A. Saffari, and A. Mahmoodian, "Various approaches in optimization of multi effects distillation desalination systems using a hybrid meta-heuristic optimization tool," *Desalination*, vol. 254, pp. 138–148, 2010.
[41] I. J. Esfahani, A. Ataei, K. V. Shetty, T. S. Oh, J. H. Park, and C. K. Yoo, "Modeling and genetic algorithm-based multi-objective optimization of the MED-TVC desalination system," *Desalination*, vol. 292, pp. 87–104, 2012.
[42] A. Piacentino, "Application of advanced thermodynamics, thermoeconomics and exergy costing to a Multiple Effect Distillation plant: In-depth analysis of cost formation process," *Desalination*, vol. 371, pp. 88–103, 2015.
[43] K. S. Pitzer and G. Mayorga, "Thermodynamics of Electrolytes. I I. Activity and Osmotic Coefficients for Strong Electrolytes with One or Both Ions Univalent," *The Journal of Physical Chemistry*, vol. 77, no. 19, pp. 2300–2308, 1973.
[44] M. Bialik, P. Sedin, and H. Theliander, "Boiling Point Rise Calculations in Sodium Salt Solutions," *Ind. Eng. Chem. Res.*, vol. 47, pp. 1283–1287, 2008.
[45] ESDU, "Condensation inside tubes: pressure drop in straight horizontal tubes," *ESDU Series on Heat Transfer*, 1993.
[46] S. Shen, "Thermodynamic Losses in Multi-effect Distillation Process," *Materials Science and Engineering*, vol. 88, pp. 1–12, 2015.
[47] H. El-Dessouky, I. Alatiqi, S. Bingulac, and H. Ettouney, "Steady-State Analysis of the Multiple Effect Evaporation Desalination Process," *Chem. Eng. Technol.*, vol. 21, no. 5, pp. 437–451, 1998.
[48] A. S. Hassan and M. A. Darwish, "Performarce of thermal vapor compression," *Desalinationn*, vol. 335, pp. 41–46, 2014.
[49] S. Lemmens, "Cost Engineering Techniques and Their Applicability for Cost Estimation of Organic Rankine Cycle Systems," *Energies*, vol. 9, no. 485, 2016.
[50] S. Georgiu, N. Shah, and C. N. Markides, "A thermo-economic analysis and comparison of pumped-thermal and liquidair electricity storage systems," *Applied Energy*, vol. 226, pp. 1119–1133, 2018.
[51] Z. Han, P. Li, X. Han, Z. Mei, and Z. Wang, "Thermo-Economic Performance Analysis of a Regenerative Superheating Organic Rankine Cycle for Waste Heat Recovery," *Energies*, vol. 10, no. 1593, 2017.
[52] R. Turton, R. C. Bailie, W. B. Whiting, J. A. Shaeiwitz, and D. Bhattacharyya, *Analysis, Synthesis and Design of Chemical Processes*. Prentice Hall, 2012.

[53] M. Z. Stijepovic and P. Linke, "Optimal waste heat recovery and reuse in industrial zones," *Energy*, vol. 36, pp. 4019–4031, 2011.
[54] A. K. Kralj, P. Glavic, and M. Krajnc, "Waste heat integration between processes," *Applied Thermal Engineering*, vol. 22, pp. 1259–1269, 2002.
[55] O. A. Hamed, "Overview of hybrid desalination systems — current status and future prospects," *Desalination*, vol. 186, pp. 207–214, 2005.
[56] H. T. El-Dessouki and H. M. Ettouney, *Fundamentals of Salt Water Desalination*. Elsevier, 2002.
[57] T. Laukemann, R. Baten, and T. Fichter, "MENA Regional Water Outlook, Phase II, Desalination using Renewable Energy," *Fichtner and DLR*, 2012.
[58] M. Micari, M. Moser, A. Cipollina, M. Bevacqua, A. Tamburini, B. Fuchs, and G. Micale, "Combined Membrane and Thermal Desalination Processes for the Treatment of Ion Exchange Resins Spent Brine," in *13th Conference on Sustainable Development of Energy, Water and Environmental systems*, 2018.
[59] S. Shen, S. Zhou, Y. Yang, L. Yang, and X. Liu, "Study of steam parameters on the performance of a TVC-MED desalination plant," *Desalination and Water Treatment*, vol. 33, pp. 300–308, 2011.
[60] M. Papapetrou, G. Micale, G. Zaragoza, and G. Kosmadakis, "Assessment of methodologies and data used to calculate desalination costs," *Desalination*, vol. 419, pp. 8–19, 2017.
[61] J. Gebel and S. Yüce, *An Engineer's Guide to Desalination.* VBG PowerTech, 2008.
[62] B. Ortega-Delgado, L. Garcia-Rodriguez, and D. C. Alarcon-Padilla, "Opportunities of improvement of the MED seawater desalination process by pretreatments allowing high-temperature operation," *Desalination and Water Treatment,*, vol. 97, pp. 94–108, 2017.
[63] M. H. Sharqawy, J. H. Lienhard V, and S. M. Zubair, "The thermophysical properties of seawater: A review of existing correlations and data," *Desalination and Water Treatment*, vol. 16, pp. 354–380, 2010.
[64] C. Sommariva, *Desalination and Advanced Water Treatment-Economics and Financing*. Balaban Desalination Publications, 2010.
[65] M. Moser, F. Trieb, and J. Kern, "Development of a flexible tool for the integrated techno-economic assessment of renewable desalination plants," *Desalination and Water Treatment*, vol. 76, pp. 53–70, 2017.

Supplementary Material

Technical model validation

The described model was validated through the comparison with another model, which is present in literature [62]. The two models are similar in their structure, both of them are employed as design models in which the areas of the heat exchangers and of the preheaters are imposed equal. Moreover, the thermo-physical properties of the salt solutions are estimated as functions of temperature and composition. The main differences consist in the estimation of the Boiling Point Elevation (BPE), which is estimated through the Pitzer model in the present model, in order to be able to cover a wider range of feed and brine salinity. Conversely, in the reference model the correlation reported by Sharqawy et al. for seawater is used [63]. This last correlation and the Pitzer model shows a good agreement at low concentrations, although the BPE calculated via the Pitzer model is higher, while at concentrations higher than 120 g/kg the correlation by Sharqawy is not valid. Also the programming method is different, since the present model is implemented in Python and a suitable resolution algorithm had to be developed, while the model by Ortega-Delgado et al. is implemented in Engineering Equation Solver (EES) and a simultaneous solver system is employed, which uses the Newton-Raphson method. For validation purposes, the models were tested within the typical desalination range of concentration (35,000-65,000 ppm) and some simulation analyses, varying the number of effects and the distillate flow rate, were carried out, both for the Forward Feed and for the Parallel Cross arrangement. For sake of brevity, only the results of the analysis performed varying N for the forward-feed MED-TVC system are reported. The inputs used for this analysis are reported in Table S 1.

Table S 1. Inputs for the reported validation analysis (variation of $N_{effects}$)

X_{feed} [ppm]	35,000
X_{brine} [ppm]	65,000
N [-]	variable (4-15)
T_{steam} [°C]	70
$P_{motive\ steam}$ [bar]	3.5
T_n [°C]	38
M_{feed} [kg/s]	5

Figure S 1 shows a very good agreement between the two models. The slight difference at higher number of effects is due to the fact that the BPE estimated in the Python model through the Pitzer equations is always higher than the one estimated in the EES model. This determines a slight difference in the areas especially at higher number of effects, where the operating ΔT of each effect is lower. As the number of effects increases, the specific area increases because of the depletion of the driving force, which is available for the single effect. At the same time, the higher the number of effects, the higher the thermal efficiency of the system. Therefore, the required motive steam decreases and the GOR increases with N.

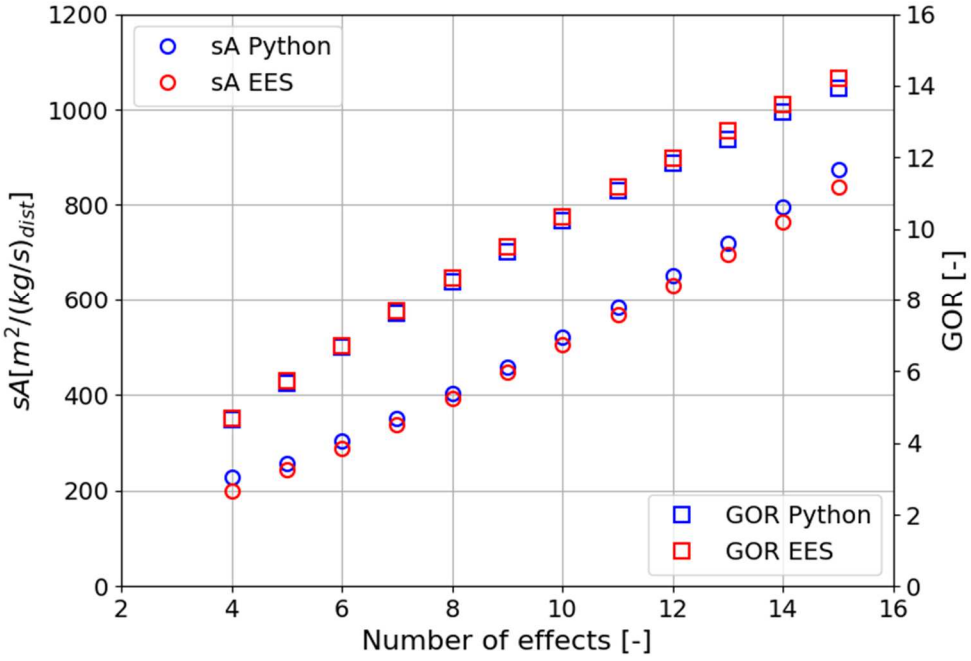

Figure S 1. Comparison of the specific area [$m^2/(kg/s)_{dist}$] and the GOR [-] as functions of the number of effects for the present model (Python model) and for the reference model (EES model) for the case of a MED-TVC system with a forward-feed arrangement.

Reference Cycle Method

The reference cycle concept as described in [64] is a simplified method for the pricing of steam extraction from a conventional steam turbine in the case of dual purpose applications, i.e. whenever electrical as well as thermal power are simultaneously produced. The key idea behind the concept is that the steam which is extracted from the turbine at a certain temperature and pressure (e.g. typically in the range of 0.3 - 2.5 bar for thermal desalination) could be further expanded in the low-pressure section of the turbine and thus generate an additional amount of electrical power. The level of further expansion is defined by the

selected cooling type (i.e. dry cooling, wet cooling or once-through cooling) and is strongly dependent on the local climatic conditions (air and water temperature and eventually air humidity). The plant in which 100% of the steam is used for electricity generation is referred as reference cycle. The price of the heat for dual-purpose applications is calculated based on the missed revenues, which could have been achieved by selling electricity in the reference cycle. Figure S 2 shows the electricity losses in kWh_{el}/ton of steam as a function of the pressure of extraction. The lines on the secondary y-axis present the heat cost assuming a conventional or a concentrated solar thermal power plant (CSP), respectively.

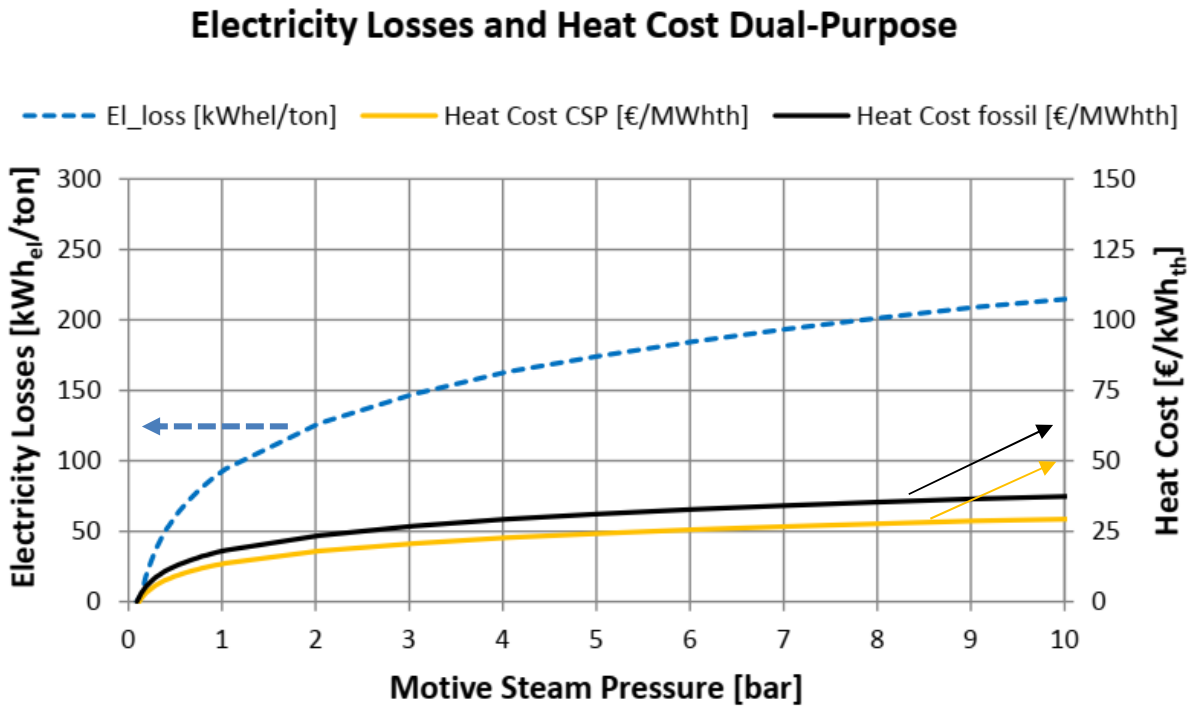

Figure S 2. Specific electricity losses (in kWh_{el} per ton of feed steam) and heat costs for a CSP plant and a fossil power plant; Assumptions: state-of-the-art CSP investment costs; fossil fuel price: 100 $/bbl [65]**.**